ON

DEEP INELASTIC MUON AND ELECTRON SCATTERING

Organiser: H Meyer, U.C. Santa Cruz and DESY

EXPERIMENTAL TESTS OF SCALING OF THE PROTON ELECTROMAGNETIC STRUCTURE FUNCTIONS*

Presented by J I Friedman

A. Bodek, M. Breidenbach, D.L. Dubin, J.E. Elias, J.I. Friedman, H.W. Kendall, J.S. Poucher, E.M. Riordan, and M.R. Sogard

Physics Department and Laboratory for Nuclear Science
Massachusetts Institute of Technology, Cambridge, Massachusetts 02139

D.H. Coward and D.J. Sherden

Stanford Linear Accelerator Center
Stanford University, Stanford, California 94305

We have extracted the structure functions W_1 and W_2 and the longitudinal and transverse virtual photoabsorption cross sections σ_L and σ_T from deep inelastic electron-proton scattering cross sections that were measured in two experiments [1,2] at the Stanford Linear Accelerator Center (SLAC). In the first Born approximation, the differential cross sections for the scattering of electrons of energy E to a final energy E' through an angle θ is related to W_1 and W_2, or to σ_L and σ_T by $d^2\sigma/d\Omega dE' = \sigma_M\{W_2(\nu,Q^2) + 2W_1(\nu,Q^2)\tan^2\theta/2\} = \Gamma\{\sigma_T(\nu,Q^2) + \varepsilon\sigma_L(\nu,Q^2)\}$, where σ_M is the Mott cross section, Γ is the flux of transverse virtual photons, $\nu = E - E'$, $Q^2 = 4EE'\sin^2\theta/2$, $W = (M^2 + 2M\nu - Q^2)^{\frac{1}{2}}$, $\varepsilon = \{1 + 2(1 + \nu^2/Q^2)\tan^2\theta/2\}^{-1}$, and M is the proton mass. We use the scaling variables $\omega = 2M\nu/Q^2$ and $\omega' = \omega + M^2/Q^2$. In this article, emphasis is placed on tests of scaling of $2MW_1$, νW_2, and νR, where $R = \sigma_L/\sigma_T$.

Extractions of R, W_1 and W_2 were made[3,4] at an array of the kinematic points (ν,Q^2) (with $W \geq 2$ GeV and $Q^2 \geq 1$ GeV^2) lying on constant-ω contours. We have tested[4] scaling in $\xi = \omega$ or ω' by fitting functions of the form $F_i = g_i(\xi)\{1-2Q^2/\Lambda_i^2\}$, to the data for $F_1 = 2MW_1$ and $F_2 = \nu W_2$. The results for Λ_1^2 and Λ_2^2 are insensitive to the choice of the functional forms for g_1 and g_2. In the $1.5 \leq \omega \leq 3.0$ ($2 \leq Q^2 \leq 15$ GeV^2) F_1 and F_2 show deviations from scaling in ω which are characterized by $2/\Lambda_1^2 = 0.0324 \pm 0.0048$ GeV^{-2} ($\Lambda_1^2 = 62 \pm 9$ GeV^2) and $2/\Lambda_2^2 = 0.0268 \pm 0.0026$ GeV^{-2} ($\Lambda_2^2 = 75 \pm 7$ GeV^2). In this same region, possible deviations from scaling in ω' are small, as indicated by the best fit values $2/\Lambda_1^2 = 0.0098 \pm 0.0070$ GeV^{-2} and $2/\Lambda_2^2 = 0.0040 \pm 0.0036$ GeV^{-2}. The quoted errors include estimated systematic uncertainties.

Deviations from scaling in ω, suggested by a number of theoretical models 5-7, were further examined[4] by fitting functions with explicit Q^2-dependent terms to F_1 and F_2 for fixed ω in the range $1.5 \leq \omega \leq 3.0$ with $2.0 \leq Q^2 \leq 15.0$ GeV^2. Best fit parameters of these Q^2-dependent terms are presented in Table I; quoted errors include estimated systematic uncertainties. The forms $F_i = a_i\left[1 - 2Q^2/\Lambda_i^2\right]$ and $F_i = a_i / \left[1 + Q^2/\bar{\Lambda}_i^2\right]^2$ arise in parton structure models.[5,6] The latter form would also result from the exchange of a heavy photon [7]. The quantities Λ_i^2 and $\bar{\Lambda}_i^2$ are given in units of GeV^2. Fits of the form $F_i = a_i\left[1 + d_iM^2/Q^2\right]$ provide a comparison of the data with a

*Work supported by the U.S. Atomic Energy Commission under contract numbers AT(11-1)-3069 and AT(04-3)-515.

$1/Q^2$ approach to scaling. The best fit coefficients d_i are close to what would be expected if the F_i scaled in ω'.

Due to the limited Q^2 range, it is unclear whether the data favor models predicting deviations from scaling in ω or models in which the asymptotic scaling values are gradually approached from above.

Figure 1 shows νR plotted versus Q^2 for fixed ω. The solid lines represent least-square fits of the form $\nu R = a + b\nu = a + (\frac{\omega}{2M})bQ^2$. We expect b = 0, i.e. νR scales, if the proton had purely spin $\frac{1}{2}$ constituents[8]; otherwise b > 0 if charged spin 0 or spin 1 constituents are also present[9]. Best fit values of B and its systematic uncertainty Δb are given in Table II for the ten values of ω studied[3]. For $\omega \leq 5$, b is small and consistent with zero, indicative of predominantly spin $\frac{1}{2}$ constituents. For $\omega > 5$, b may be different from zero, but the data for these ω lie in a small range of low Q^2 and a nonzero b might reflect only the low-Q^2 threshold behavior of R.

The constant value $R = 0.16 \pm 0.10$ provides a better fit than $R = Q^2/\nu^2$ to all the data[3] for R. An even better fit is obtained with the form[9] $R = f(\omega)Q^2/\nu^2$ where $f(\omega) = g\omega^2$, with $g = 0.13 \pm 0.07$. Quoted errors in these numbers include the estimated systematic uncertainties[3]. This deviation from Q^2/ν^2 behavior[9] at large ω is apparent in Figure 1 where the dashed lines represent $R = Q^2/\nu^2$.

Using inelastic e-d cross-sections[1], R for the neutron and R for the deuteron were found[3] to be equal to R for the proton, within the statistical errors. Recent measurements[10] of the neutron to proton cross-section ratio, σ_n/σ_p, have extended the earlier studies[1] to higher values of Q^2 and lower values of ω. The quantity σ_n/σ_p falls monotically with decreasing ω but the values still lie above the quark model lower bound of 0.25.

References

1. A. Bodek et al., Phys. Rev. Lett. 30, 1087(1973).
2. J.S. Poucher et al., Phys. Rev. Lett. 32, 118 (1974).
3. E.M. Riordan et al., SLAC-PUB-1417 (1974), to be published in Phys. Rev. Letters.
4. A. Bodek et al., SLAC-PUB-1442 (1974).
5. M.S. Chanowitz and S.D. Drell, Phys. Rev. D9, 2078 (1974).
6. G.B. West and P. Zerwas, SLAC-PUB-1420 (1974).
7. T.D. Lee and G.C. Wick, Nucl. Phys. B9, 209 (1969).
8. J.E. Mandula, Phys. Rev. D8, 328 (1973).
9. J.F. Gunion and R.L. Jaffe, Phys. Rev. D8, 3215 (1973); C.G. Callan and D.J. Gross, Phys. Rev. Lett. 22, 156 (1969).
10. A Bodek et al., SLAC-PUB-1399 (1974), to be published in Physics Letters.

Table I

$F_i = a_i\left[1 - 2Q^2/\Lambda_i^2\right]$ $\quad F_i = a_i/\left[1 + Q^2/\bar{\Lambda}_i^2\right]^2$ $\quad F_i = a_i\left[1 + d_i M^2/Q^2\right]$

ω	Λ_1^2	Λ_2^2	$\bar{\Lambda}_1^2$	$\bar{\Lambda}_2^2$	d_1	d_2
1.50	59±15	71±16	24±14	45±20	13.73±12.73	4.84±2.66
1.75	68±19	59± 9	40±20	39±11	3.83±3.02	2.59±0.86
2.00	58±10	74±14	36±11	55±14	2.96±1.15	1.29±0.37
2.50	67±21	89±19	52±21	66±16	0.90±0.40	0.48±0.11
3.00	59±19	120±59	47±24	107±59	0.70±0.44	0.31±0.17

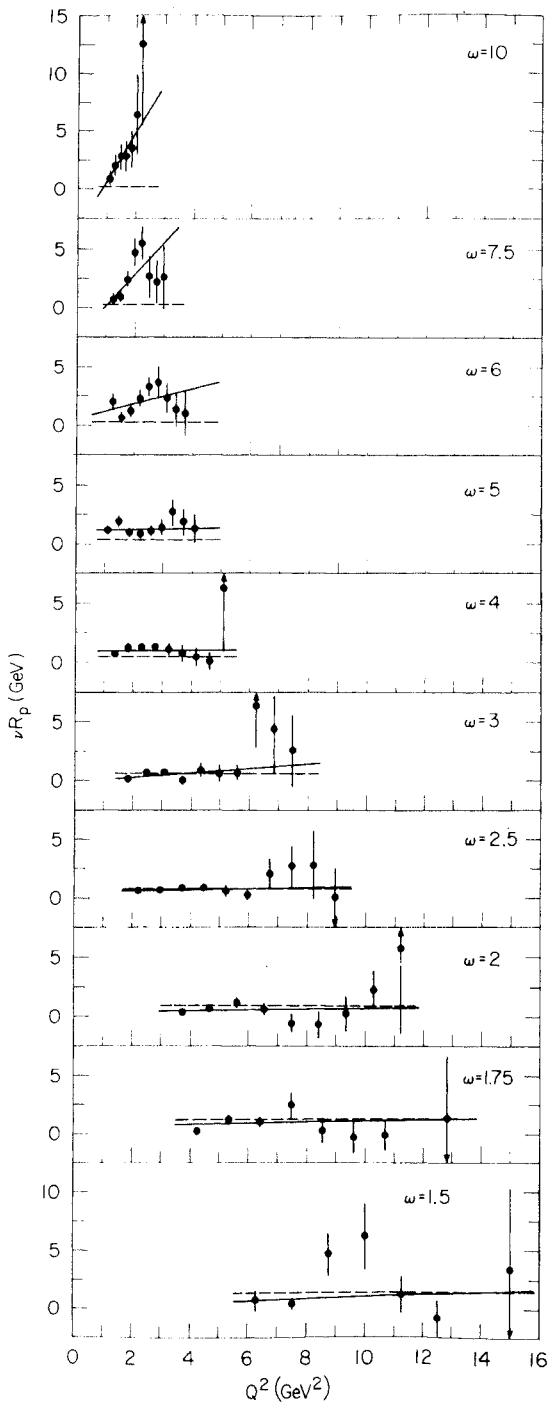

Fig. 1 νR plotted vs. Q^2 for fixed ω. The solid curves represent fits of the form $\nu R = a + b\nu \equiv a + \frac{\omega}{2M} b\, Q^2$. The dashed lines represent $R = Q^2/\nu^2$.

Table II

ω	b	Δb
1.50	0.11±0.28	0.14
1.75	0.02±0.15	0.08
2.00	0.04±0.10	0.06
2.50	0.03±0.07	0.06
3.00	0.12±0.07	0.07
4.00	0.02±0.07	0.06
5.00	0.02±0.09	0.08
6.00	0.20±0.13	0.12
7.50	0.66±0.19	0.17
10.00	0.80±0.31	0.18

PRELIMINARY RESULTS FROM A RECENT EXPERIMENT ON INCLUSIVE DEEP INELASTIC SCATTERING*

Presented by R E Taylor

W.B. Atwood, E.D. Bloom, R.L.A. Cottrell, H. Destaebler, M. Mestayer, C.Y. Prescott, L.S. Rochester, S. Stein, R.E. Taylor, D. Trines†

Stanford Linear Accelerator Center,
Stanford University, Stanford, California 94305.

In a recent experiment at SLAC, we have made more measurements of single-arm deep inelastic electron scattering cross sections from liquid hydrogen and deuterium targets. Investigations at large angles, 50° and 60°, were made using the 1.6 GeV spectrometer with a new counter system designed to detect electrons. Additional measurements in kinematic regions covered in previous experiments have been made using the 20 GeV spectrometer system. At the large angles the backgrounds (largely due to pion production) are severe, and π-e separation must be better than ten-thousand to one. In the 1.6 GeV spectrometer, discrimination between π's and electrons was accomplished using a threshold Cerenkov counter and lead glass counters divided into four segments of 1.2, 4, 9 and 9 radiation lengths. By placing cuts on the pulse height signals from these counters, we were able to achieve a rejection ratio of $\sim 5 \times 10^4$ with an electron efficiency of 96%, leaving less than ~5% π contamination in the electron signal for those kinematics corresponding to maximum background. Corrections for the remaining 5% are made on a statistical basis, as the π-component energy spectrum has a different shape than that for electrons. The experiment is otherwise similar to the previous work at SLAC, with a target of 17.6 cm - somewhat larger than usual to increase the rates at large angles.

* Work supported by the U.S. Atomic Energy Commission.

† Present Address: I. Physikalisches Institut der Rheinisch Westfalischen Technischen Hochschule Aachen, 51 Aachen 1, Schinkelstr. 2, West Germany.

Analysis of the data is just beginning, and we have only fragmentary results to present to the Conference. We have some results from a comparison of electron and positron scattering from hydrogen. Positrons were made in a radiator one-third of the way along the accelerator and accelerated to 13.9 GeV in the remaining two-thirds of the machine. Beams of ~1% of the electron intensity are obtainable in this way. By changing the phase of the last two-thirds of the accelerator, electrons of the same energy can be obtained from the same radiator, or 13.9 GeV electrons can be obtained from the accelerator gun in the usual way. Some kinds of systematic error might cancel when electrons and positrons are produced in the same radiator, but no significant differences in the two sorts of electrons were detected. The cross sections for the two signs of incident particle were obtained in the 20 and 1.6 GeV spectrometers. Data were taken at several values of W and Q^2 as shown in Fig. 1. The ratio of the cross sections for positrons and electrons scattering is shown in Fig. 2. The inner hatch marks on the error bars show the size of the statistical errors. Systematic errors clearly dominate in the preliminary analysis and may be reduced as the analysis proceeds. No corrections to the data for radiative processes have been applied to the data. Note that the cross sections ratio is mainly sensitive to the difference in radiative corrections between e^+p and e^-p.

The absence of significant differences between e^+ and e^- cross sections over the range of Q^2 is an encouraging indication that one-photon processes play a dominant role in deep inelastic scattering (although a difference would measure only the real part of an

interference term between one and two-photon processes).

These results may also have implications for models which speculate on the existence of new short range direct lepton-hadron interactions.[1,2,3] Such models might explain the large e^+e^- annihilation cross sections which have recently been observed. Some of these models predict substantial differences between $\sigma(e^+p)$ and $\sigma(e^-p)$ for regions of kinematics covered in the present experiment and are, therefore, not favoured by the data. Note that the absence of e^+e^- differences does not rule out this class of model, as examples exist which predict no e^+e^- differences. In a communication to the Trieste Conference, Professor E.D. Bloom has summarized the constraints imposed on such models by deep inelastic scattering experiments.

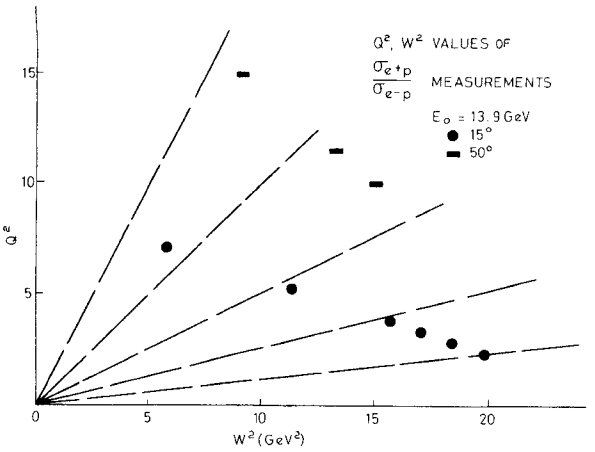

Fig. 1

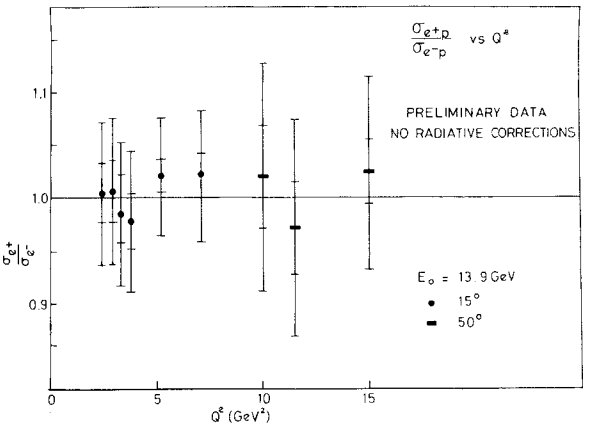

Fig. 2

REFERENCES

1. B Richter and M Breidenbach, private communication.
2. J C Pati and A Salam, Phys. Rev. Lett. 32(1974)1083
3. I Y Bigi and J D Bjorken, SLAC-PUB-1422(May 1974).

TEST OF SCALE INVARIANCE IN HIGH ENERGY MUON INTERACTIONS*

Michigan State University - Cornell University - UC San Diego - Collaboration

Presented by L N Hand

D.J. Fox+, C. Chang, K.W. Chen, A. Kotlewski,
P.F. Kunz†
Michigan State University, East Lansing, Michigan 48823

L.N. Hand, S. Herb, S.C. Loken, A. Russell, Y. Watanabe
Cornell University, Ithaca, New York 14850

W. Vernon
University of California at San Diego, La Jolla,
California 92037.

M. Strovink**
Princeton University, Princeton, New Jersey 08540

It is of interest to test the concept of scale invariance at the higher energies now available at the Fermi National Accelerator Laboratory in order to see whether the apparent point-like nature of the constituents is maintained with the shorter distances resolved at these higher energies.

* Supported by National Science Foundation Grants GP 59070, GP 32565, and GP 28317.

+ Deceased.

† Now at Stanford Linear Accelerator Center, Stanford, California 94305.

** Visiting Assistant Professor, Cornell University, 1971-72. Now at the Univ. of California, Berkley, California 94720.

In the experiment reported here, 56.3 and 150 GeV muons are scattered from an iron target and momentum analyzed using a spectrometer consisting of magnetized iron toroids. The scaling test is made by comparing measured distributions in q^2 at these two incident muon energies, or by separate comparison with Monte Carlo predictions based on the SLAC results. Although it is necessary in principle to assume the form of R in order to interpret the results, in practice it makes little difference. A method was devised which compensates for variation of the kinematic range accepted by the spectrometer through simultaneous variation of the apparatus geometry with the beam energy. Requiring both the acceptance region and spectrometer multiple scattering to be nearly identical at all measured points along the scattered muon trajectory essentially determines both the geometric configuration and the ratio of the two incident energies. It is possible to satisfy all of these conditions everywhere only because $\frac{\sqrt{3}}{3} = \frac{\sqrt{8}}{5}$ to about 2%. The relative energies are then in the ratio 3:8 as is the amount of scattering material, while the actual bending power, i.e. magnetized part of the spectrometer, changes in the ratio 3:5. To a large extent this design for the apparatus makes it possible to minimize variations in the acceptance and "edge" effects due to scattering in or out of the finite spectrometer aperture.

It should be emphasized that the scaling test reported here uses an iron target. Thus additivity is an assumption made when comparing the data in this experiment to the predicitons based on Monte Carlo calculations.

A scattered muon trigger is defined by three counter banks having a hole in the center to prevent beam triggers. A fourth bank of counters is placed upstream of the target to veto accidental beam-halo coincidences. The beam size at the target is sharply defined by another veto counter. Beam muons or muons scattered through very small angles are vetoed by a coincidence of two veto counters labelled BV and BV' in Fig. 1. To prevent an accidental vetoing of real events the holes in each magnet are plugged with concrete.

A multiwire proportional counter system is used both to record the incident beam track and to locate the scattered track immediately downstream of the target. The beam track is located to ±1.5mm with the incident angle measured to ±0.1 mrad.

For some events, typically having a very high energy loss ν, the scattered muon track may be obscured by a hadronic or electromagnetic shower. To provide information on these events the target is segmented into 4-inch blocks with scintillation counters between each block. The pulse height in these counters is recorded and will ultimately be used to provide additional information on the location of the event vertex. In the results reported here only information from the spark chambers located downstream of the first magnet in the spectrometer is used. The other information can be used to improve the spectrometer resolution.

Data was taken in August and October 1973 (150 GeV) and April 1974 (56 GeV). The results reported here are based on about 30% of the total data sample and only one position of the target. In the single target position used for the data reported here the q^2 range for an acceptance greater than 10% is <5 to more than 50 $(GeV/c)^2$. The mean ω value is about 9 and the mean q^2 about 14 $(GeV/c)^2$. The effective number of muons for the present data is approximately 0.80×10^9 at 150 GeV and 1.7×10^9 at 56 GeV. 98% of the

150 GeV beam and 91% of the 56 GeV beam is contained with a 9 cm radius and 2 milliradian divergence angle. In some of the data, notably the 150/56 ratio comparison, a 4.5 cm 1 milliradian beam cut was used. This provides a further reduction in the effective total flux to 0.43 and 1.0×10^9 at 150 and 56 GeV respectively. The beam spill was such that on the average about 5% of the events contained two beam tracks. Corrections were made to the flux for veto dead time and loss in reconstructing proportional chamber beam tracks (a few percent in each case). The data rate (reconstructed events) was observed to remain constant over instantaneous beam intensities varying over at least one decade.

It was useful to trigger on beam tracks selected at random to monitor the beam geometrical characteristics and to provide an input sample to Monte Carlo simulations of the experiment. Periodically the beam was steered into the spectrometer to provide calibration data.

The momentum fit takes into account multiple scattering and measurement errors and allows for error correlations between track positions measured in different modules.

To check the absolute reconstruction efficiency, the number of events expected in the same q^2,ω range as that covered by SLAC was computed and compared with the number actually obtained, normalized to the effective muon flux. The ratio of predicted events/observed events was 1.00±0.05 at 150 GeV and 0.89±0.07 at 56 GeV.

As a measure of any observed violation of scale invariance, we can parameterize a hypothetical violation by assuming:

$$F_2(q^2,\omega) = \frac{N}{(1 + q^2/\Lambda^2)^2} F_2 \text{ (SLAC)}$$ where the function F_2(SLAC) is derived from fits to the electron scattering data and scales (is a function only of ω at these energies). Λ has the dimensions of a mass and provides a scale. Varying N allows us to vary the absolute normalization of the muon experiment relative to the SLAC electron scattering data. No inference should be drawn concerning the actual validity of the above functional form for F_2

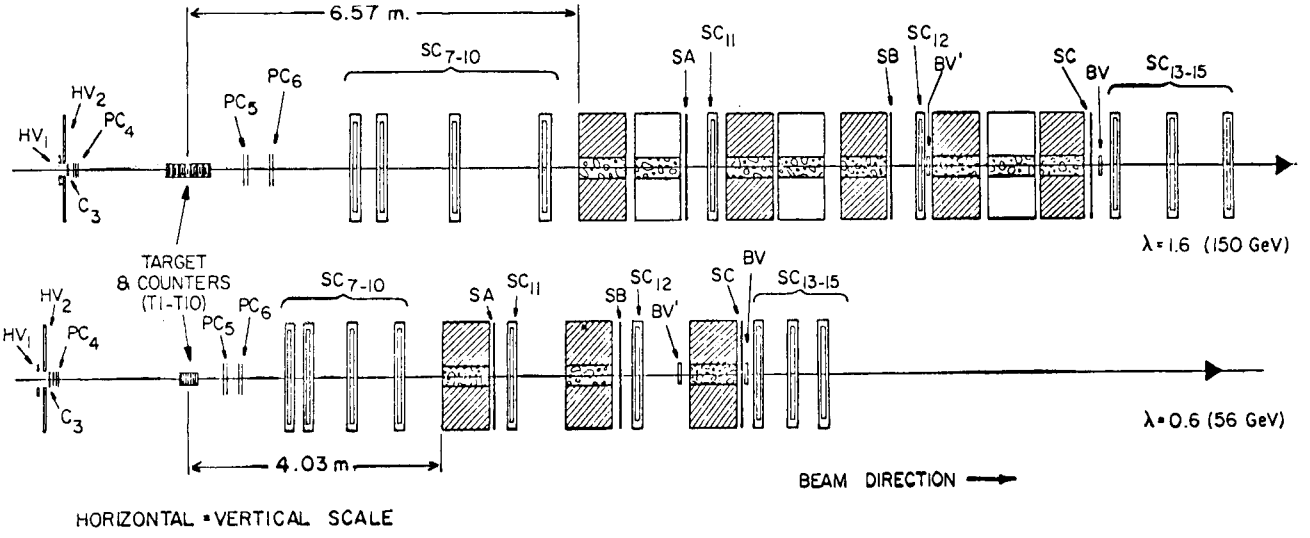

Fig. 1 Apparatus used for the scaling test. SC = spark chamber; PC = proportional chamber; SA, SB, SC = counter hodoscope; HV, BV = veto counters.

which is merely a convenient way of expressing the degree of scale breaking in the experiment. In particular, it should be noted that ω(or x) varies across the q^2 distribution plotted in Fig. 2 due to our experimental acceptance, thus making it difficult to distinguish possible types of scale breaking from each other given this information alone.

The main results of this experiment to date are plotted in Fig. 2 and the results of fits of the type discussed above are given in Table I. We see that the data to Monte Carlo comparison shows a statistically significant deviation from the extrapolated values expected using the hypothesis of scale invariance and the SLAC F_2 values. The tendency of the normalization to be greater than 1.0 probably indicates that the functional form of the deviation is not a correct description of the physical effects being observed, particularly since good agreement is obtained with the absolute normalization in the region overlapping the SLAC kinematic range. Very poor fits are obtained by either assuming $1/A^2 = 0$ or N = 1.0.

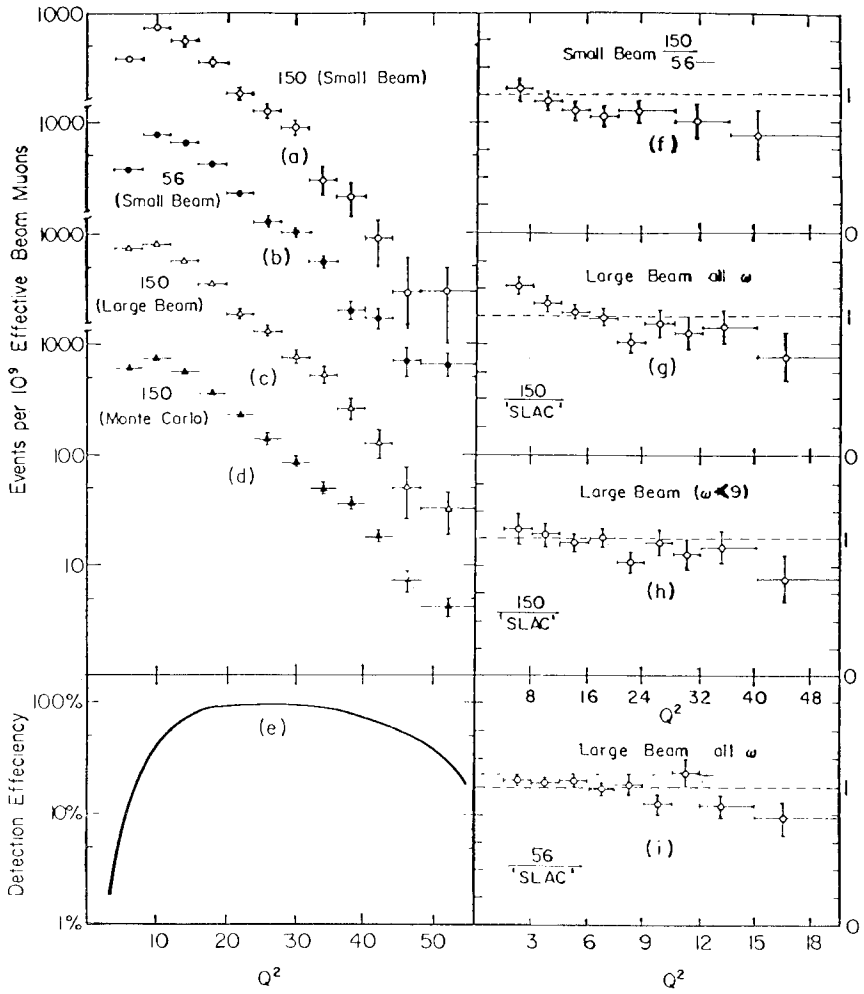

Fig. 2 a) - d) Observed Q^2 distributions. 'Small beam' indicates radius $\leq$ 4.5 cm, divergence $\leq$ 1.0 mr cut in the data. e) detection efficiency plotted vs Q^2. f - i) results of comparison between 56 GeV data and 150 GeV data and of comparison of each separately with Monte Carlo simulation.

We note that if a cut is made to restrict the data to $\omega < 9$, a less rapid decrease with q^2 is observed.

The systematic errors in this type of comparison are estimated to be ~ 0.0030 $(GeV/c)^{-2}$ in $1/\Lambda^2$ and $\pm 10\%$ in the normalization. By taking the ratio of 150 GeV data to 56 GeV data we can eliminate the need to depend on the Monte Carlo calculation at the price of losing statistical accuracy. The radiative corrections, absolute reconstruction efficiency, exact shape of F_2 in iron all cancel out along with other purely experimental effects. Using this method we obtain a $1/\Lambda^2$ about 2 standard deviations from 0. This method is presently limited by statistics.

Table 1. Results of Fits to Data in Fig.2

	Data Sample	Ref. Fig. 8	N	$\frac{1}{\Lambda^2}$ in $(GeV/c)^{-2}$	χ^2/n_D	Confidence Level	Remarks
Absolute = $\frac{\text{Data}}{\text{Monte Carlo}}$	150 GeV	g	$1.30 \pm .06$	$.0083 \pm .0015$	5.5/7	61%	
	150 Gev, $\omega < 9$	h	$1.10 \begin{smallmatrix}+.10\\-.06\end{smallmatrix}$	$.0042 \begin{smallmatrix}-.0015\\+.0028\end{smallmatrix}$	3.5/7	83%	"Loose" Beam
	56 GeV	i	$1.10 \pm .03$	$.0110 (\sim \pm .0020)$	7/7	44%	
	150 GeV/56 GeV	f	$1.10 \pm .10$	$.0120 \pm .0060$	1.1/5	94%	"Tight" Beam No corrections Note χ^2 is low
Ratio = $\frac{\text{Data}}{\text{Data}}$	150 GeV/56 GeV	g,i	$1.20 \begin{smallmatrix}+.10\\-.07\end{smallmatrix}$	$.0106 \begin{smallmatrix}+.0060\\-.0040\end{smallmatrix}$	7.8/7	37%	"Loose" Beam, Correction from ratio of Monte Carlos at 56 and 150 GeV
			$0.997 \pm .028$	0	15.3/8	12%	Fit to a constant

FINAL-STATE FEATURES IN DEEPLY INELASTIC ELECTRO-AND MUOPRODUCTION*

Clemens A Heusch

University of California, Santa Cruz, California

We seek to cover the following four points:

1. What happens to the final-state hadrons as the exchanged photon becomes more massive (Q^2 increases)?
2. Do individual final-state channels account significantly for global features observed (like, for instance, $R = \sigma_L/\sigma_T$ and the forward charge ratio n^+/n_-)?
3. Do final-state features favor any particular model in a decisive way?
4. What experimental progress is there in the leptoproduction of hadrons?

On points 1 through 3, there are some very recent results which I want to discuss. They are from two streamer chamber experiments with good statistics, and were submitted to this conference:

DESY,[1] 7.2 GeV electrons (where the experiment has been reported on in the past)[2]; and

UC Santa Cruz - SLAC,[3] 14.2 GeV μ^+ (where results are being reported for the first time).

These are the only high-statistics studies that fully observe all charged final-state hadrons. A hybrid bubble chamber experiment at SLAC[4] has given exploratory information. The kinematical range will

*Supported in part by the United States Atomic Energy Commission under Contract AT(04-3)-34, P.A. 197.

soon be extended greatly by the NAL-Chicago-Harvard experiment, where, however, momentum analysis and track delineation will be partial.

Let me then start with point 4, and give a few details on the newly reported Santa Cruz-SLAC experiment: To make up for disadvantages caused by the SLAC duty cycle limitations, a very high quality muon beam of reasonable intensity was built[5]. The muons originate from asymmetric pair production by bremsstrahlung photons in heavy materials (Cu, Au), where only small transverse momenta are introduced:

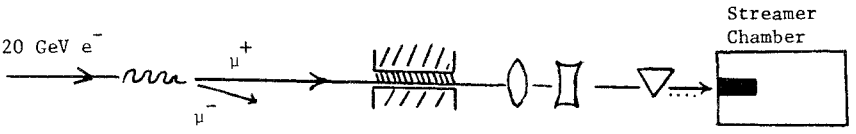

The well-defined final beam is obtained at considerable expense: one muon into the final acceptance needs $\sim 10^9$ electrons to be fully accelerated by SLAC. Here are the beam parameters:

$E_{(\mu^+)} = 14.2$ GeV	divergence ~ 2 mrad
flux $\leq 10^5$/sec	halo $\simeq 1\%$
$\frac{\Delta p}{p} = \pm 1\%$	pion contamination = $(4 \pm 1.5)10^{-5}$
beam spot $\simeq 1 \times 1$ cm^2	

Schematically, the beam is described in Fig. 1a.[5] Fig. 1b shows the experimental setup: a 40 cm long liquid hydrogen target is surrounded by a 2 m long streamer chamber of cross-section .8 X .6 m^2, all inside a 16 kG magnetic field. Veto walls upstream and a 1.5 m Pb wall allow a clean trigger for muons scattered out of the beam phase space. A Cherenkov monitor downstream provides normalization to 1-2%. Fig. 1c gives a few details on the techniques used to allow the passage of several hundred muons per memory time through the streamer chamber,[6] where liquid hydrogen plus the heavy chamber gas might create forbidding δ ray problems: the target is surrounded by a re-entrant cavity filled with inert gas, with teflon fins above and below the target to intercept electrons spiralling along the field lines; and non-scattered muons will exit downstream through a He-filled lexan tube, ~ 5 cm wide. The geometrical inefficiencies thus introduced are unimportant. The δ ray ("flare") occurrence was thus reduced to a level that created minimal problems for scanning and measuring of some 250,000 pictures taken in 3 views (15° stereoscopy).

Now to the data: first, the most distinct final state,

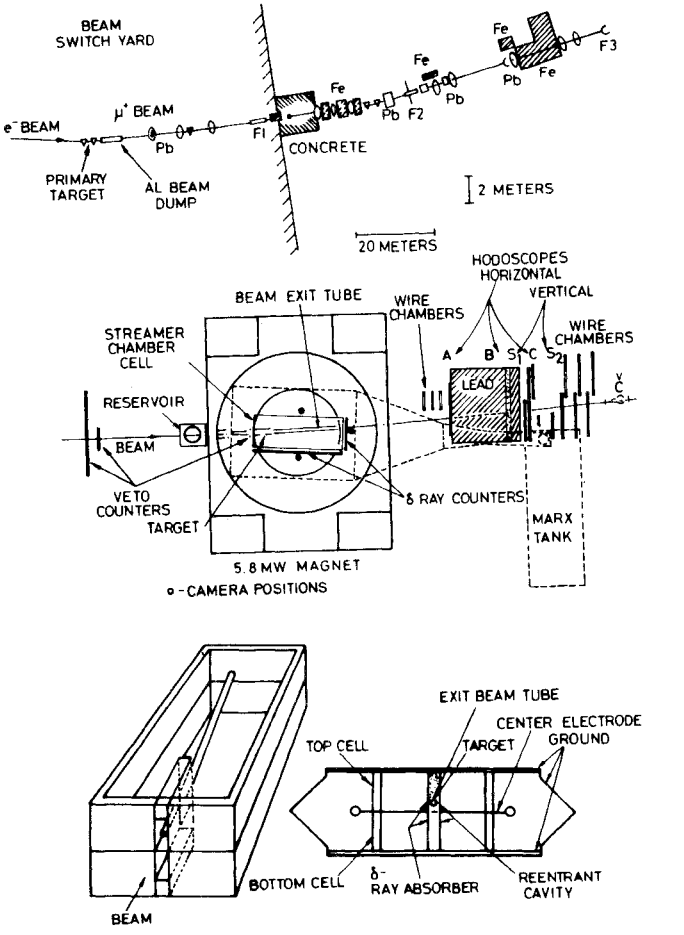

Fig. 1 The muon beam, experimental set-up and details of the streamer chamber.

elastic scattering. Fig. 2 gives evidence that up to $Q^2 = 1$ the dipole fit and normalization from ep scattering closely resemble what is seen here. Eventually, these data (where radiative corrections have yet to be applied) will allow a precision comparison of μp and ep scattering to at least an honest 5% level. Let us now revert to questions 1 through 3.

What happens to hadron distributions when we go to a comprehensive study of all channels? From ∿ 40% of their data, the Santa Cruz-SLAC Group reports prong distributions and muon charged multiplicities up to Q^2 values of about 3. Fig. 3a gives the fraction of one-hadronic prong events over the total (the muon is never counted as a prong), with the dashed line indicating the photoproduction ($Q^2 = 0$) value for comparison. This class of events, which contains such channels as

$$\gamma_v p \rightarrow \pi^+ n \ (+\pi^o \ldots)$$
$$\rightarrow \pi^o p \ (+\pi^o \ldots),$$

is clearly much more important for $Q^2 > 0$ than for $Q^2 = 0$ in all energy bins shown here except in the lowest, where isobars are expected to be important. The corresponding graph for 3 charged hadrons shows the opposite trend (Fig. 3b): here, photoproduction shows a higher fraction in all but the lowest s bins. Remember that this fractional cross section contains:

$$\gamma_v p \rightarrow \rho^o p \ (\rho^o \rightarrow \pi^+\pi^-)$$
$$\rightarrow \omega^o p \ (\omega^o \rightarrow \pi^+\pi^-\pi^o)$$
$$\rightarrow \phi^o p \ (\phi^o \rightarrow K^+K^-)$$

in addition to $\gamma_v p \rightarrow \pi^- \Delta^{++}$, $\pi^+ \Delta^o$ ($\Delta \rightarrow N\pi$).

The well-known decrease of σ_ρ/σ_{tot} with Q^2 will therefore be reflected here. In Fig. 3c, the fractional five-prong cross-section is shown (containing, at higher W, e.g., $\rho' \rightarrow 4\pi$ production): it is similar for $Q^2 > 0$ as for $Q^2 = 0$.

The outstanding feature in all of these data is the apparent independence of Q^2 for all $Q^2 > 0$ values reported here. Fig. 4 shows the same feature for the average charged multiplicity; again, with better statistics, there is no Q^2 dependence in the range covered.[7]

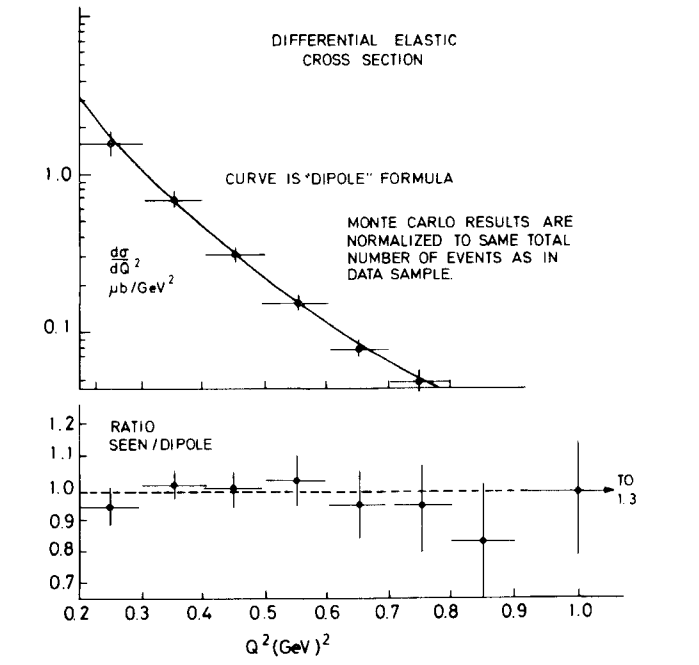

Fig. 2 Measured elastic μp scattering compared with expectations from the dipole formula (SLAC-UCSC data).

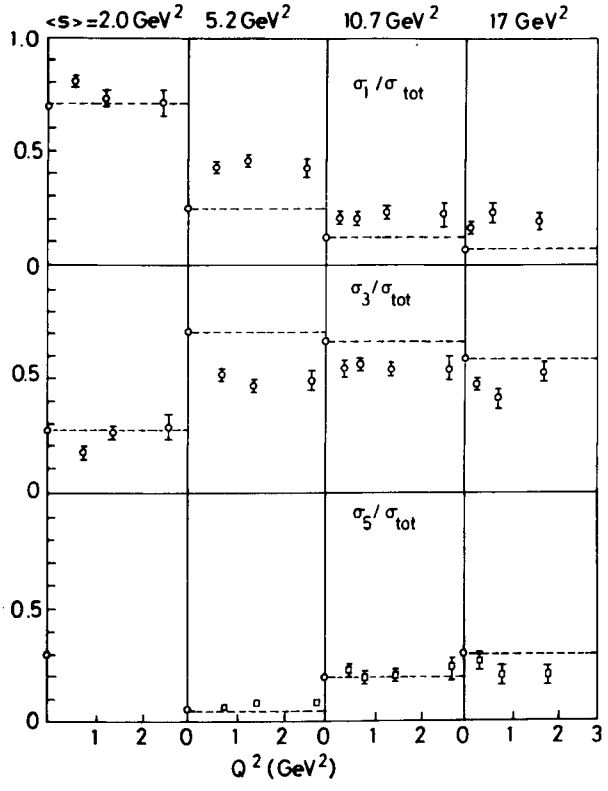

Fig. 3 a,b,c Cross-sections for 1, 3 and 5 charged hadrons, as a fraction of the total cross section, versus Q^2.

What is the mean charged multiplicity as a function of energy? Fig. 5 shows the new data to be easily described by a linear dependence with ln s, with a slope very similar to photoproduction (slope of ~ 1), but a lower intercept. This is in serious conflict with data recently reported by a Cornell group[8], whose counter experiment indicated a negative intercept and a slope of ~ 1.5 (also indicated in Fig. 5) for the same mean Q^2 value of ~ 1.4).

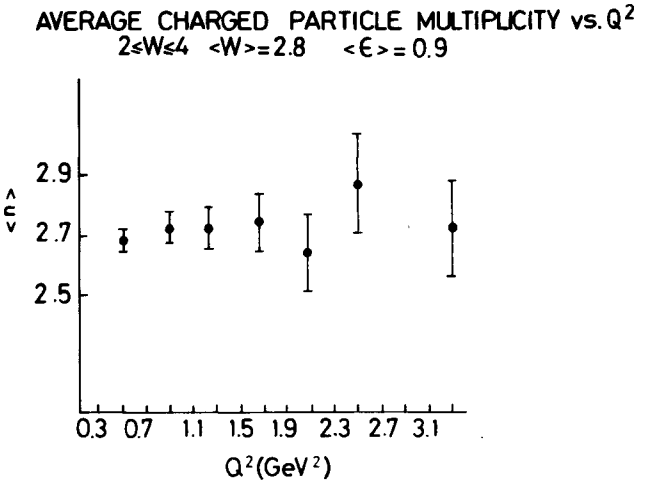

Fig. 4

We now turn to individual hadronic channels. When all final-state particles are charged, we can do reliable four-constraint (4C) fits. A detailed analysis submitted by the DESY group studies the states contained in

$$\gamma_v p \rightarrow \pi^+\pi^- p,$$

i.e., mostly ρ^o and Δ^{++}, Δ^o production. Let us see what Q^2 effects we can follow up on in these reaction mechanisms.

For the reaction

$$\gamma_v p \rightarrow \Delta^{++}\pi^-,$$

the data were compared to the "electric Born term model" formulated originally by Stichel and Scholz[9] for photoproduction, in a modification to electroproduction that is due to Bartl et al.[10] The DESY group contends that the angular distribution and the decay matrix elements of the Δ support the notion that, close to threshold, the "contact term"

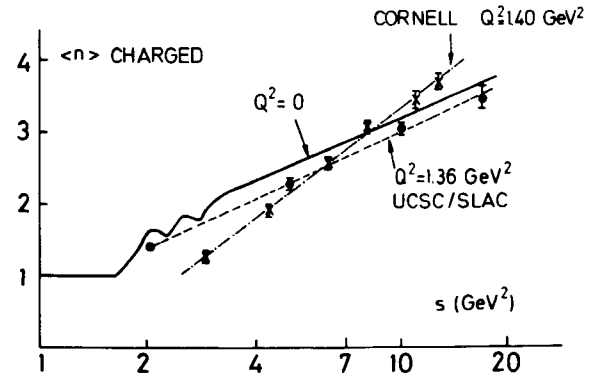

Fig. 5 Mean charged multiplicity as a function of energy.

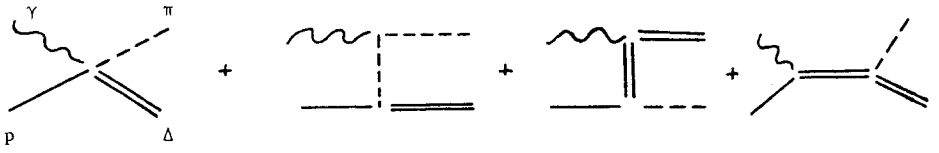

dominates for transverse photons. A rapid fall-off with Q^2, quantitatively described by a substitution of the photon propagator

$$\frac{1}{Q^2} \rightarrow \frac{1}{Q^2 + m_\rho^2}$$

by the (VDM-inspired) ρ propagator, gives reasonable agreement with the data trend (Fig. 6). Fig. 7 shows that, to describe the energy trend, a strong absorption correction has to quash the influence of the contact term soon above threshold.[11]

Of more concern at higher energy is the channel

$$\gamma_v p \rightarrow \rho^o p,$$

for which the vector dominance model has postulated paramount importance, and past experiments have claimed a great diversity of results. Both the DESY and the Santa Cruz-SLAC results show a prominent ρ content in their sample of $\pi^+\pi^-p$ final states by a maximum-likelihood method; it is seen that this content (σ_ρ/σ_{tot}) diminishes rapidly as Q^2 increases in the (low) W region covered by DESY. Again, a ρ-propagator-type Q^2 dependence, modified by the factor $\xi = R\, m_\rho^2/Q^2$ (where R is determined by assuming s-channel helicity conservation (SCHC) and using the ρ decay data) is seen (Fig. 8) to be compatible with the experimental trend.

Is there evidence for "photon shrinking" in the slope parameters for the "diffractive" forward peak in

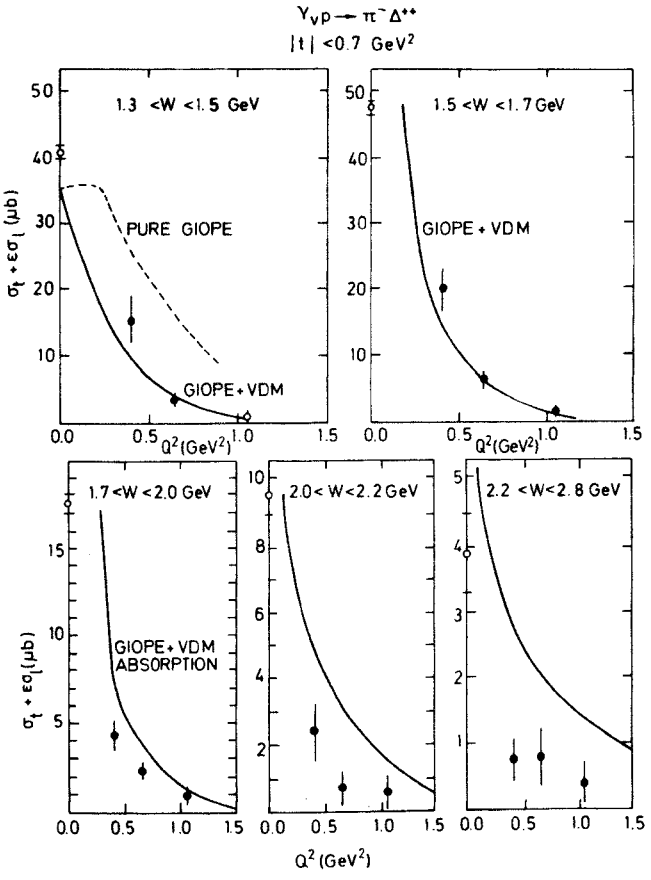

Fig. 6 Reaction $\gamma_v p \to \pi^- \Delta^{++}$. The solid (dashed) line is the prediction of the Born term model with (without) a ρ - propagator factor. Absorption is included at higher W. (Data from DESY).

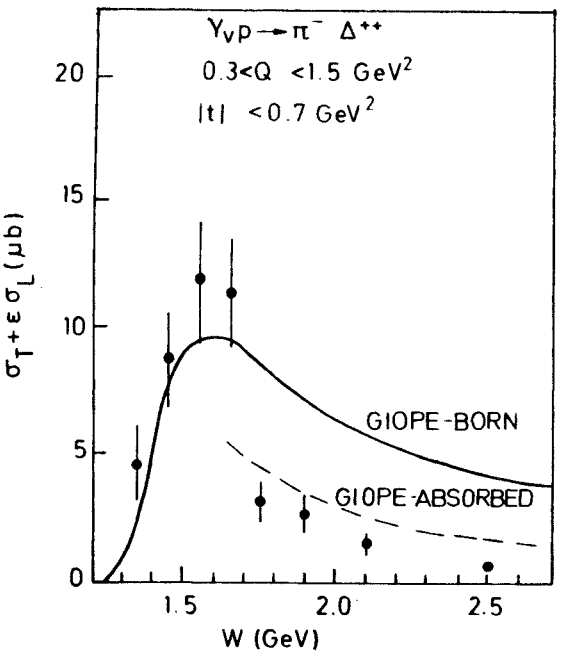

Fig. 7 Cross section for $\gamma_v p \to \pi^- \Delta^{++}$ as function of W. The solid curve is the prediction of the Born term model modified by vector dominance. The dashed curve includes absorption corrections. (Data from DESY).

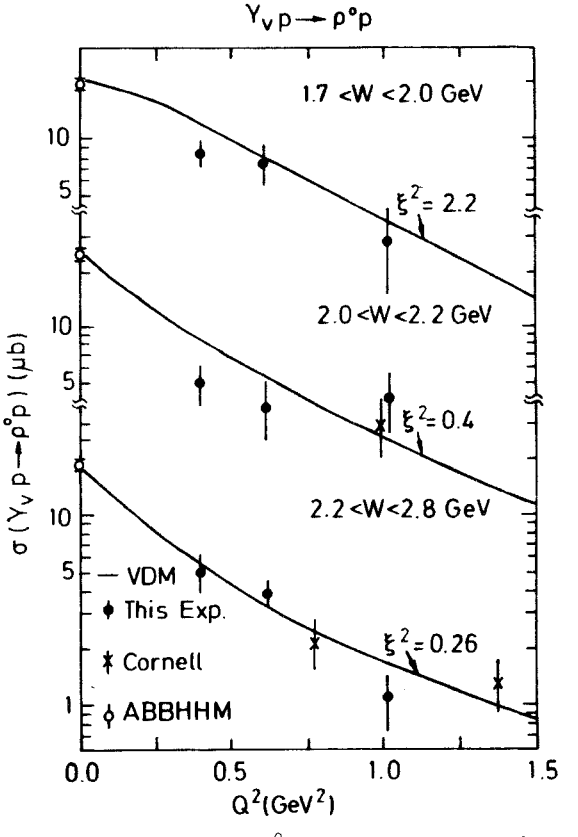

Fig. 8 Reaction $\gamma_v p \to \rho^0 p$: total cross section as function of Q^2 for different W intervals (DESY - U. of Hamburg data). The Cornell data also shown (Alrens et al.) has had the ω contribution subtracted. The curve is a vector dominance prediction.

$\frac{d\sigma}{dt}$ ($\gamma_v p \rightarrow \rho p$) $\sim e^{bt}$?

The careful DESY analysis yields an instructive picture (Fig. 9): for small Q^2 (between 0.3 and 0.5) and larger values (0.5 - 1.5), these peaks are compared with the photoproduction peak, and the question remains entirely open. All previous claims for a flattening of the forward peak ought to be re-examined in this light: between what t values do you fit to an exponential? What W and Q^2 bins should be defined? How background-affected is that sample? Photon shrinking is clearly a problem to be attached by higher-energy experiment (the Santa Cruz-SLAC analysis expects results soon, at Q^2 values out to ~ 3).

From their analysis of the ρ^0 decay matrix elements, the DESY group see possible evidence for a 5% helicity flip admixture in the data. If, in this framework, we assume SCHC to hold, then Fig. 10 shows that the longitudinal photon contribution to the cross-section is considerable close to threshold ($R = \sigma_L/\sigma_T$), but decreases soon to a value around 0.2. The parameter cos δ, a measure for longitudinal/transverse interference (for natural spin-parity exchange) indicates minimal interference around threshold, but a trend towards in-phase behavior at $W \geq 4$. This may be taken as an indication that, at higher energies, both σ_L and σ_T become predominantly diffractive. Clearly, similar probes for the photon's behavior could be provided by the other vector mesons. However, beyond reporting indications for observation of ω^0, ϕ^0 mesons in their final states (Fig. 11), the Santa Cruz-SLAC collaboration leaves these points for future publication of presently ongoing work.[12]

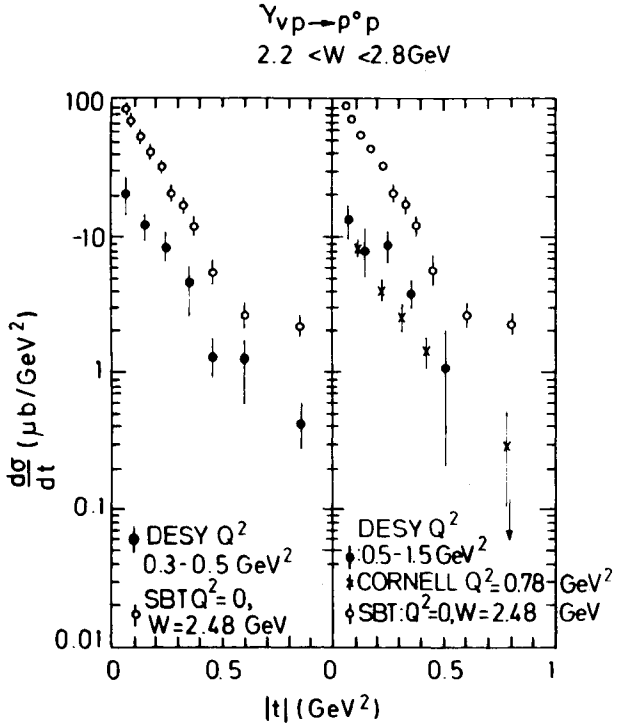

Fig. 9 Differential cross section for $\gamma_v p \rightarrow \rho^0 p$ in two Q^2 ranges. The Cornell data has had the ω contribution subtracted. Photoproduction data of the SBT collaboration is also shown.

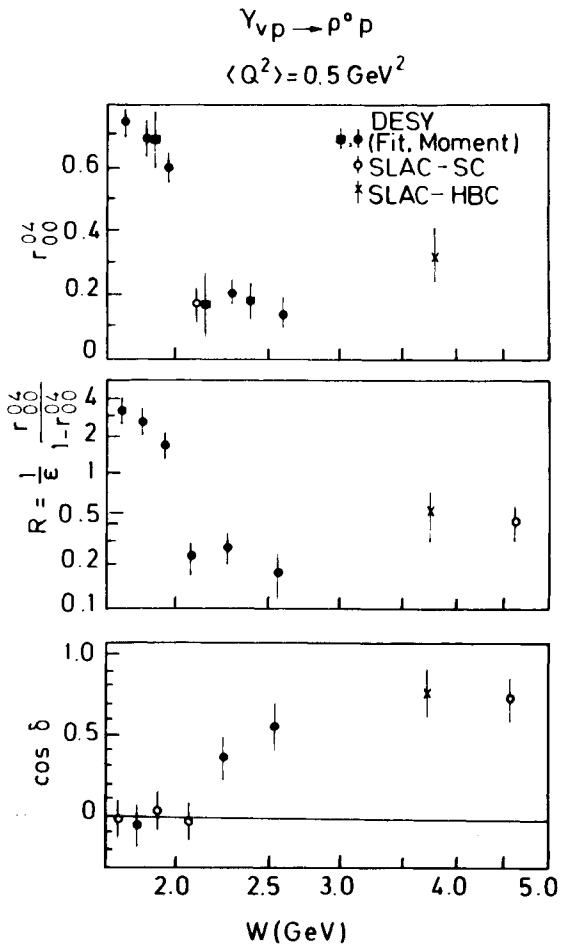

Fig. 10 Reaction $\gamma_v p \rightarrow \rho^0 p$: density matrix element r_{00}^{04}, $R = \sigma_L/\sigma_T$ (calculated assuming SCHC) and cos δ (phase between transverse and longitudinal production calculated assuming only natural parity exchange).

Conclusions:

We sum up our progress report; prominent features are these:

1) σ_1 (cross-sections for production of one charged hadron in the final state) is higher for virtual than real photons at all energies above the nucleon isobar region;
   σ_3 is lower for Q > 0.1 than at $Q^2 = 0$ at energies above the isobar region;
   σ_5 is roughly equal for electro- and photo-production.
2) <n> is lower for $Q^2 > 0.1$ than for $Q^2 = 0$.
3) <n> (average number of charged hadrons is linear with ln s, with a slope close to that observed in photoproduction.
4) <n>, σ_1, σ_3, σ_5 are independent of Q^2 for $Q^2 >$ 0.1.
5) The 4C channel $\gamma_v p \rightarrow \pi^+\pi^- p$ shows clear signals for ρ, Δ^{++} production.
6) For the $\pi^-\Delta^{++}$ channel, the "electric Born model", modified by the introduction of a ρ propagator into the "contact term", plus absorption corrections, is compatible with Q^2 and W dependence.
7) ρ production: disappears fast with Q^2; slope of forward peak has ill-determined Q^2 dependence; "photon shrinking" is poorly established.
8) Longitudinal component is strong close to threshold, then decreases rapidly towards R values of ~ 0.2.
9) σ_L may become diffractive with increasing energy.

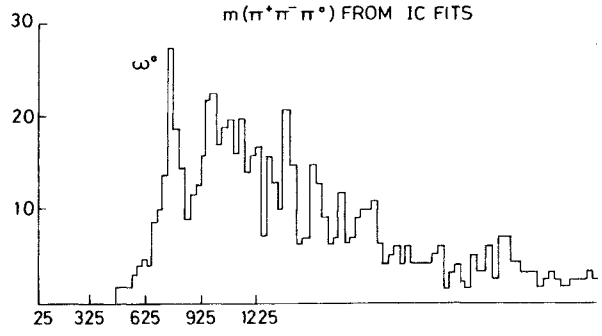

Fig. 11

References

1) P. Joos et al., Paper 392, this Conference.
2) V. Eckardt et al., Nuclear Physics B55, 45 (1973).
3) K. Bunnell et al., Papers 207, 208, this Conference.
4) J. Ballam et al., SLAC-PUB-1373 (1974).
5) S. Flatte, C. Heusch, A. Seiden, Nuc. Inst. Methods, to be published, UCSC 74-01 (1974).
6) C. Heusch, B. Lieberman, A. Seidan, Nuc. Inst. Methods, to be published, UCSC 72-016 (1974).
7) Similar behavior was observed in other investigations, although graphs containing information from different experiments showed sizable Q^2 effects (see Ref. 8).
8) B. Gibbard et al., Cornell preprint CLNS-266(1974).
9) P. Stichel, M. Scholz, Nuovo Cimento 34, 1381 (1964).
10) A. Bartl, W. Majerotto, D. Schildknecht, DESY 72/4 (1972).
11) Interest in the contact term, particularly its Q^2 dependence, has been rekindled by the recent $e^+e^- \rightarrow$ hadron data. See C. Ferro-Fontan, H. Rubinstein, CERN-TH 1810 (1974).
12) Other features of the Santa Cruz-SLAC data are discussed in the report of Martin Perl to this Conference.

REVIEW OF INCLUSIVE PION ELECTROPRODUCTION

M L Perl

Stanford Linear Accelerator Center

1. This review is based on the following papers presented to this Conference:

Paper 160, J.T. Dakin et al, SLAC; electroproduction on hydrogen and deuterium using spark chambers.

Papers 207 -209, K. Bunnell et al, Univ. of California at Santa Cruz and SLAC, muonproduction on hydrogen using a streamer chamber.

Paper 392, V. Eckardt et al, DESY and Universitat Hamburg; electroproduction on hydrogen using a streamer chamber.

Paper 575, C.J. Bebek et al, Harvard Univ.; electroproduction on hydrogen and deuterium using a double arm spectrometer.

The incident lepton energies ranged from 7 to 20 GeV. No inclusive electroproduction or muonproduction data was available at higher energies. Unless otherwise noted the data is from a proton target.

2. Inclusive Distributions: ϕ and x dependence

(a) Using $\dot{\sigma}(q^2,\nu) = d^2\sigma_{e \text{ or } \mu +N}/d\, q^2 d\nu$ Lorentz invariant cross sections for

e or μ + p → e as μ + π + anything

are defined by

$$\frac{E}{\dot{\sigma}(q^2,\nu)} \frac{d^3\dot{\sigma}(q^2,\nu)}{d^3\,\vec{p}} = \frac{2E^*}{\dot{\sigma}(q^2,\nu)} \frac{d^3\dot{\sigma}}{d\,p_{\parallel}^{\,*} dp_\perp^{\,2} d\phi}$$

E^*, $p^*_{\parallel}$, $p_\perp$ and ϕ refer to the pion in the virtual photon-nucleon barycentric system, relative to the virtual photon direction. We define $x = p^*_{\parallel}/p^*_{max}$.

(b) The ϕ dependence has the general form

$1 + C_{\underline{p}}\, \varepsilon \cos 2\phi + \sqrt{2\varepsilon(\varepsilon+1)}\; C_I \cos\phi$. At lower energies (392), $C_{\underline{p}}$ (the transversely polarized photon term) is 0.40 ± 0.09; and C_I (indicating transverse-longitudinal photon interference) is -0.23 ± 0.05; both values refering to the $0.3 < x < 0.7$ region - the so-called virtual photon or beam fragmentation region. But at higher energies (160), $C_{\underline{p}}$ and C_I are $\simeq 0.1 \pm 0.1$ in the virtual photon fragmentation region. Thus the effects on the inclusive distributions of the polarization of the virtual photon decrease as the energy of the photon increases.

(c) Integrating over ϕ we define

$$F(q^2,\ \nu,\ x, p_\perp) = \frac{1}{\dot{\sigma}(q^2,\nu)} \frac{E^*}{\pi p^*_{max}} \frac{d^2\dot{\sigma}(q^2,\nu)}{d\,x\,d\,p_\perp^{\,2}}$$

(d) To study the x distributions, consider $\int_0^\infty F(q^2,\nu,x,p_\perp)dp_\perp^{\,2}$. All experiments agree with the beautiful result that $\int_0^\infty F dp_\perp^{\,2}$ is independent of q^2 and ν, if the two-body reaction $\gamma_{virtual} + p \to \rho^o + p$ is eliminated. This nice scaling law is illustrated in Fig. 1. Similar results occur for a neutron target.

3. Inclusive Distributions: $p_\perp$ dependence

(a) The dependence of F on $p_\perp$ is not so simply described because the q^2 dependence is still uncertain. F decreases rapidly as $p_\perp$ increases, so for fixed x intervals we can parameterize the data by an exponential

$$\int_{x_1}^{x_2} F\, dx = A(q^2,\nu)\; e^{-b(q^2,\nu)p_\perp^2}$$

New data (209) show that a sum of exponentials, $A_1\, e^{-b_1 p_\perp^2} + A_2\, e^{-b_2 p_\perp^2}$, is a better fit. As shown in Fig.2, the break occurs at $\approx 0.3\ p_\perp^2$

(b) Some theories predict that the effective radius of the virtual photon should decrease as $|q^2|$ increases. This could appear as a decrease in b (with increasing $|q^2|$) in the above equations when $x \gtrsim 0.2$ or so. This effect is not seen at lower energies (392), but does seem to appear at higher energies (160), particularly in π^+ production. b decreases from about 6 to about 4 $(\text{GeV/c})^{-2}$. However in view of the break in the exponential and the differences between π^+ and π^- production, more data is needed to clarify this question.

4. π^+/π^- Production Ratio in Virtual Photon Fragmentation Region

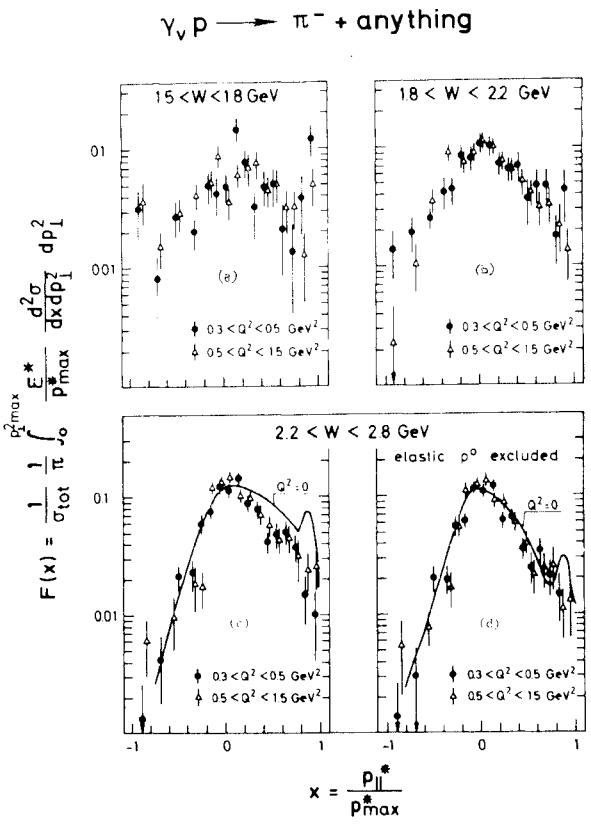

Fig.1 (a-c) Normalized structure function F(x) for inclusive π^- electroproduction for different W, Q^2 intervals.

(d) F(x) for inclsuive π^- electroproduction after removal of the ρ^0 contribution ($0.6 < M_{\pi^+\pi^-} < 0.9$ GeV in the reaction $\gamma_V p \to \pi^+\pi^- p$) for different Q^2 intervals in the W region 2.2 - 2.8 GeV.

The curves in Figs. 1d, c show the $Q^2 = 0$ result.

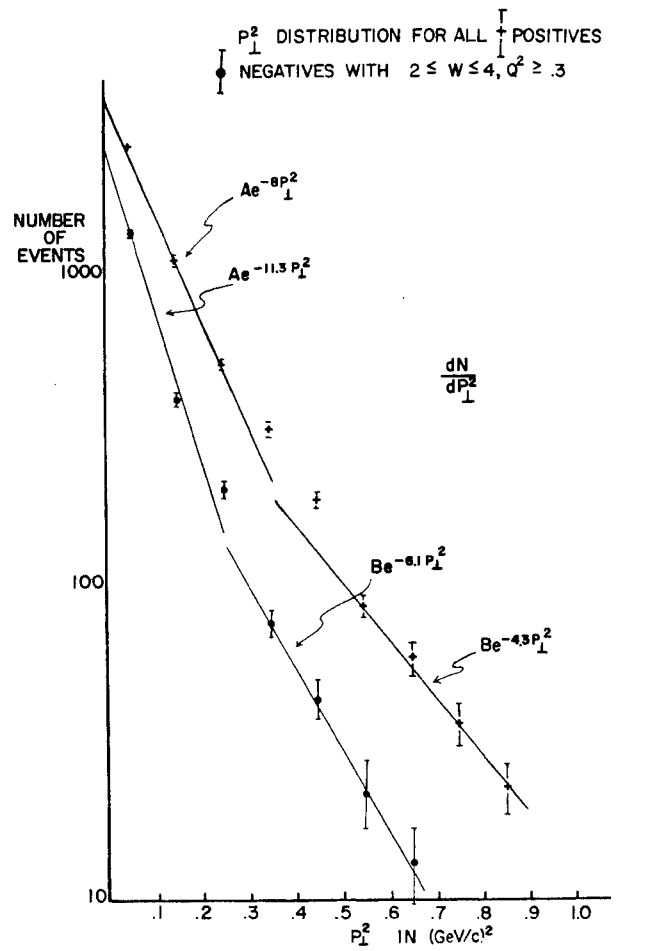

Fig.2 Figure showing $dN/dp_\perp^2$ curve from Santa Cruz-SLAC data)

(a) Consider the ratio $R_p = F_{\pi+}/F_{\pi-}$ for pions produced on a proton target in the virtual photon fragmentation region, $x \gtrsim 0.2$ or 0.3. All experiments (160, 209, 392, 575) agree with the remarkable result that R_p for virtual photons is larger than P_p for real photons; the former reaching 2 or 3 while the latter is 1.1. But the q^2 and ν dependence of this effect is not determined.

(b) As shown in Fig. 3, R_p increases with $|q^2|$, the more virtual the photon, the larger R_p.

(c) However, as shown in the upper part of Fig.4, R_p also seems to be a function of $\omega = 2M\nu/|q^2|$ only. But this could be caused by the kinematic ranges of all the experiments in which large $|q^2|$ is correlated with small ν. More data is needed.

(d) A simple quark-parton model (J.T. Dakin and G.J. Feldman, Phys. Rev. D8, 2862 (1973)) can explain the behaviour of R_p as the "pushing forward" of positive charge due to the excess of positively charged over negatively charged quarks in the proton. It is remarkable that this simple model also predicts the correct π^+/π^- ratios in neutrino-nucleon and antineutrino-nucleon production of pions, as first reported at this conference by M. Haguenauer et al (papers 512, 513).

(e) As shown in the lower part of Fig.4, the π^+/π^- ratio produced on a neutron target does not vary so clearly with ω, nor does it vary so clearly with $|q^2|$.

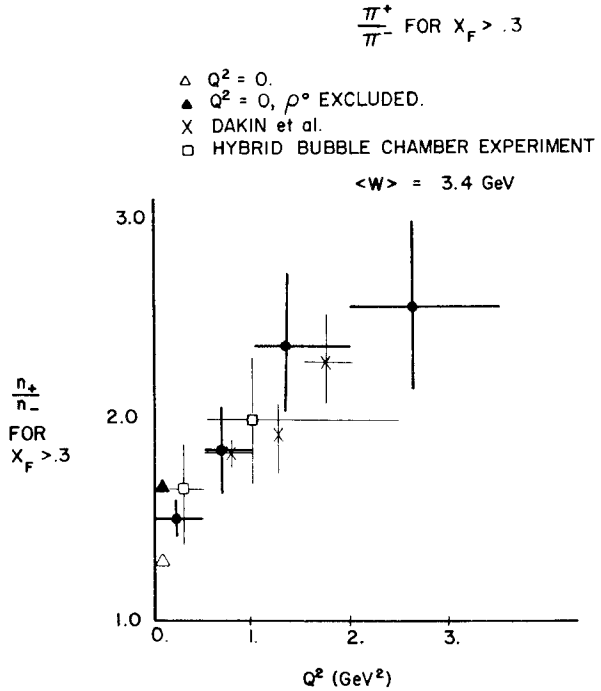

Fig.3 Figure showing π^+/π^- compilation from Heusch talk).

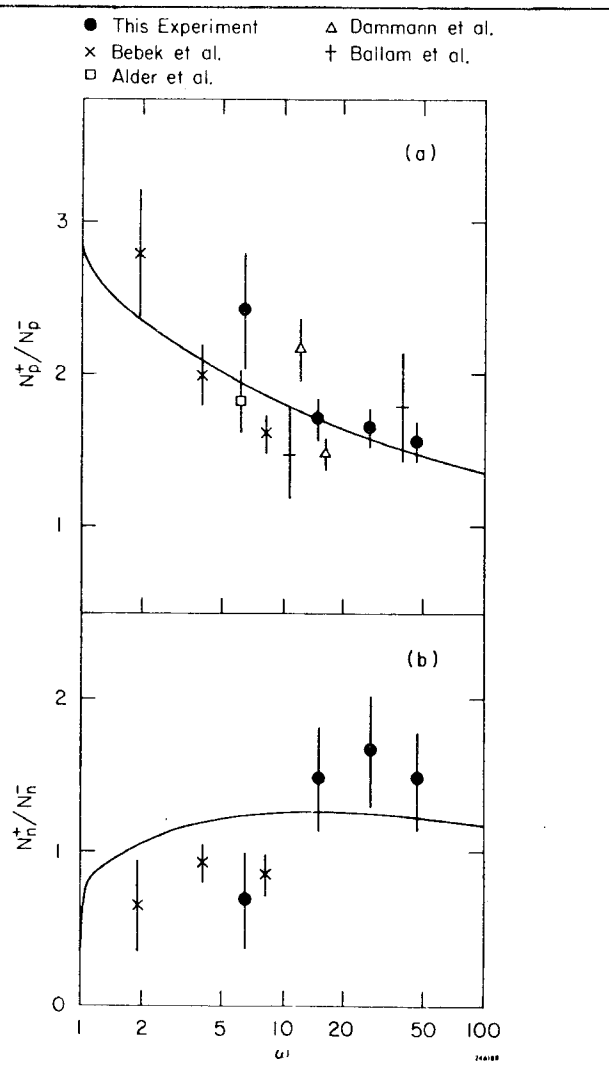

Fig.4 Particles ratios for the region $0.4 < x < 0.85$ plotted versus ω. Data are shown for (a) proton and (b) neutron targets. The curves are taken from the quark-parton model predictions of Dakin and Feldman.

INCLUSIVE ELECTROPRODUCTION OF FORWARD PROTONS FROM NEUTRON AND PROTON TARGETS

and

A MEASUREMENT OF THE PION FORM FACTOR UP TO $Q^2 = 4.0$ GeV^2*

Presented by F M Pipkin

C.J. Bebek, C.N. Brown, M. Herzlinger, S. Holmes,
C.A. Lichtenstein, F.M. Pipkin, S. Raither and
L.K. Sisterson
Harvard University, Cambridge, Mass.

We report new measurements of the inclusive electroproduction reactions

$$e^- + (p,n) \rightarrow e^- + p + \text{anything}$$

and of the exclusive reactions

$$e^- + (p,n) \rightarrow e^- + (\pi^+,\pi^-) + (n,p)$$

carried out at the Wilson Synchrotron Laboratory at Cornell University. Data were taken with deuterium at the (W,Q^2) points (2.15 GeV, 1.2 GeV^2), (2.15, 4.0) and (3.11, 1.2); data were with hydrogen at these points and at the points (2.15, 2.0), (2.67, 3.4) and (3.11, 1.7). Two magnetic spectrometers were used to detect the scattered electron and hadron. A combination of Cerenkov counters, shower counters and time of flight identified the electrons, pions, kaons and protons. The electroproduction data were treated as photoproduction by a virtual photon of mass-Q^2, energy ν and polarization parameter ϵ[1].

The proton data were analysed in terms of the invariant structure function as defined by the equation

$$F = \frac{E}{\sigma_{Tot}}\frac{d^3\sigma}{dp^3} = \frac{1}{\sigma_{Tot}}\frac{1}{\pi}\frac{E^*}{\left[p^*_{max}{}^2 - p_\perp^2\right]^{1/2}}\frac{d}{dx'dp_\perp^2}$$

Figure 1 shows the invariant structure function for $p_\perp^2 < 0.02$ GeV^2 and two values of W. The data for all the points show the following regularities: (a) the invariant structure function for protons from a neutron target is only slightly less than that for protons from a proton target; (b) the invariant structure function varies little with Q^2 at fixed W; (c) the invariant structure function decreases rapidly with W at fixed Q^2 for $x' > 0$.

The charged pion data from the deuterium target were used to determine the relative isovector (V) and isoscalar contributions to the pion electroproduction amplitude through the equation

$$R = \frac{\sigma(e+d \rightarrow e+\pi^- + p + p_s)}{\sigma(e+d \rightarrow e+\pi^+ + n + n_s)} = \frac{|V - I|^2}{|V + I|^2}$$

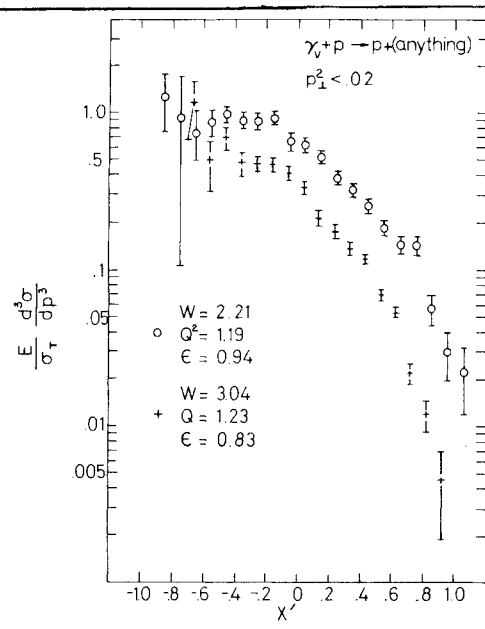

Fig. 1. Invariant structure function for $\gamma_\nu + p \rightarrow p + \text{anything}$.

* Research supported in part by U.S. Atomic Energy Commission under Contract AT(11-1)-3064.

Figure 2 shows a plot of R versus momentum transfer. A fit to the data for R was used to determine the isovector component of the hydrogen cross sections. Berends' theory was then used to determine the pion form factor[2,3]. Figure 3 shows the value of the form factor obtained using the measured R and assuming R = 1. The single pole expression

$$F_\pi = 1/(1 + Q^2/0.47)$$

gives a good fit to the data.

REFERENCES

1. C.J. Bebek et al., Phys. Rev. Lett. 30, 624 (1973).
2. F.A. Berends, Phys. Rev. D1, 2590 (1970).
3. C.J. Bebek et al., Phys. Rev. D9, 1229 (1974).

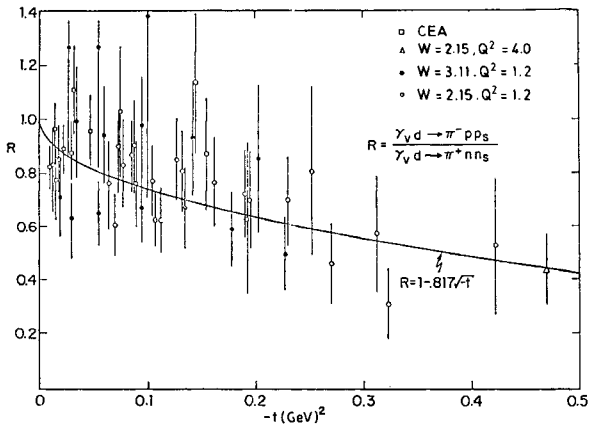

Fig. 2 A plot of the electroproduction measurements of R versus momentum transfer t.

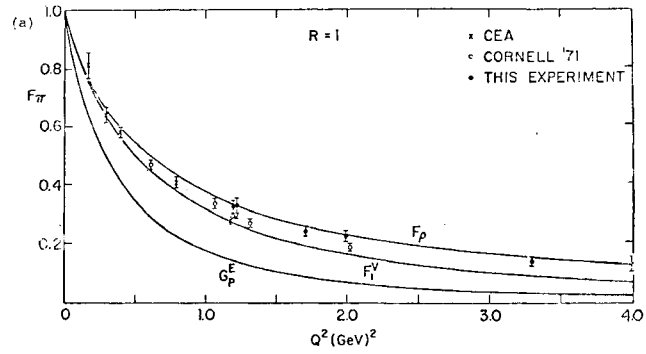

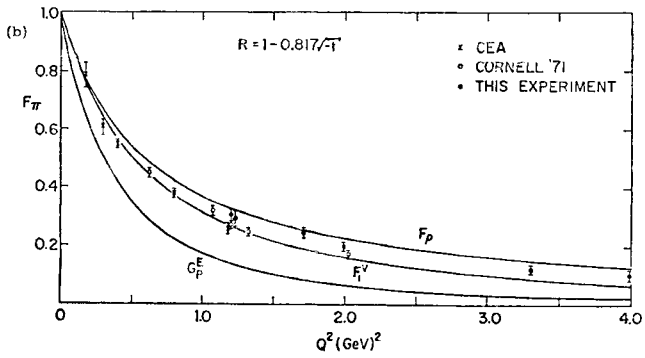

Fig. 3. The value of the pion electromagnetic form factor derived from the data using the dispersion theory of Berends, (a) for no isoscalar component and (b) for isoscalar component given by $R = 1 - 0.817\sqrt{-t}$.

INELASTIC COMPTON SCATTERING AND INCLUSIVE PHOTOPRODUCTION OF γ, π^0 AND η^0

D O Caldwell, J P Cumalat, A M Eisner, V B Elings, B N Kendall, T P McPharlin, R J Morrison, F V Murphy and B W Worster

University of California, Santa Barbara*

High energy photons from a hydrogen target bombarded by a 21-GeV bremsstrahlung beam at SLAC have been detected in an 88-counter lead-glass array, arranged in two vertically separated stacks. Because γ-γ coincidences could be measured, the experiment provides new information on inclusive γ, π^0, and η^0 photoproduction at high energies. A particular motivation for the experiment was to observe inelastic

*Supported in part by the US Atomic Energy Commission.

Compton scattering, in an attempt to measure the average charge of nucleon constituents.

An 1/8"-square positron beam of 2, 7, and 12 GeV was used to map out counter responses as a function of energy and beam position. The photon-positron difference was checked with a bremsstrahlung beam. System gains were tracked by using a light pulser, fired between beam pulses and monitored by a vacuum photodiode, feeding all counters via fiber light guides. Periodically, neutral density filters were inserted in the light pulser, enabling the deviation from linearity of each counter system to be determined. These results give mean energies to ±0.5% in scale and $\lesssim$60 MeV locally for the upper stack of shorter counters and to ±0.8% and ≤100 MeV for the lower stack of longer counters, although energy resolutions were 0.30-0.35 GeV (rms) at 12 GeV. The data have been corrected for the mean energy response of a given counter to photons incident at all possible positions and for the resolution about that mean.

Time as well as pulse-area information was digitized, and the accidental coincidence correction thus measured varied from 10% to 28%. Other corrections included: empty target rates (6%); beam attenuation in the target (1%); events lost due to timing cuts (2-5%); and energy shifts due to photon "pile-up", resulting in 5-23% excesses in yields. This last, and uncertainties in the energy scale, dominated the systematic errors.

Fig. 1 shows the π^0 photoproduction data plotted for fixed values of transverse momentum (p_T), obscuring the sharp dependence on energy (E) and angle. Statistical and representative systematic errors are shown. Photoproduction data[1] for π^+, measured for comparison with our results[2] from an earlier version of this experiment, show that the π^0/π^+ ratio is approximately constant and equal to 0.8. The curves shown are based on the constituent-interchange model,[3] using a term $\varepsilon^b/(p_T^2 + \mu^2)^a$, where $\varepsilon \simeq 1-(p/p_{max})_{cm}$, integrated over the allowed bremsstrahlung beam energies. The curves are for b = 0.6, a = 6.5, μ^2 = 0.80 GeV^2, quite close to the values b = 0-1, a = 6 for the $\bar{q}p \to qq\pi$ subprocess expected[3] to be important in the small ε region. (Our data are mainly for ε = 0 to 0.4.) The results are not consistent with the $\gamma p \to \pi q$ subprocess (a = 3-4, b = 3).

Decays of higher mass particles, such as $\eta^0 \to 2\gamma$ and $\omega^0 \to \pi^0 + \gamma$, can give coincidences between the two stacks of counters. A clear mass peak for the former is seen, and we find $(\eta^0 \to 2\gamma)/\pi^0 = (20 \pm 6.5)\%$, so that for p_T of 1-2 GeV/c about half as many η^0's as π^0's are produced. Lack of higher mass events sets a limit of $(\omega^0 \to \pi^0\gamma)/\pi^0$ of $\lesssim$ 0.5 (or $\omega^0/\pi^0 < 5$), but SLAC streamer

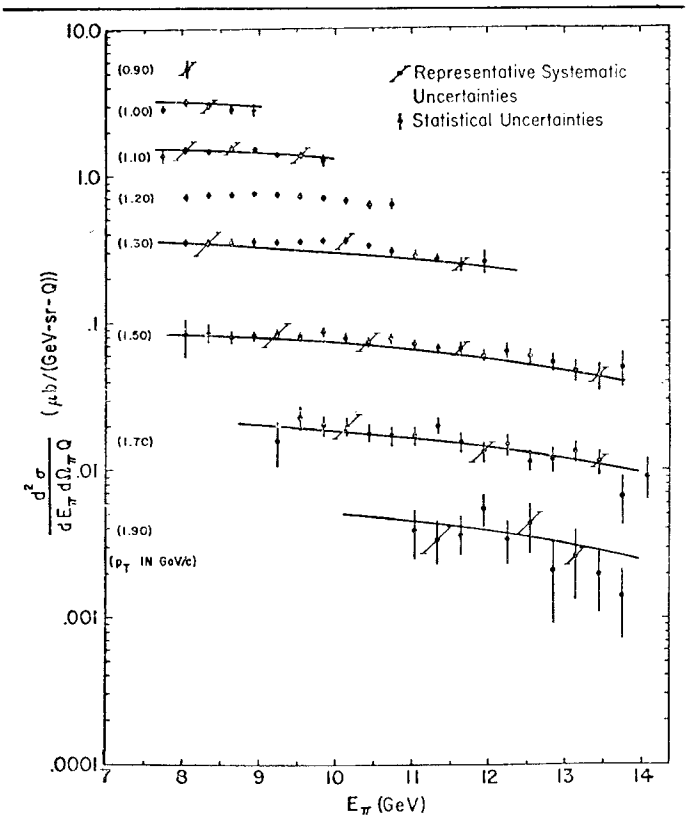

Fig. 1 π^0 photoproduction data plotted for fixed values of transverse momentum (p_T). Statistical and representative systematic errors are shown.

chamber data[4] on ρ^0 production imply an even lower limit (if $\omega \leq \rho$), and it is unlikely that such decays could contribute as much as 10% to our single γ yield.

Fig. 2 shows the single γ yield (curve A) and its form after subtracting the contributions from $\pi^0 \to 2\gamma$ and $\eta^0 \to 2\gamma$ (curve B), assuming (as is consistent with our data) that the η has the same E and p_T dependence as the π^0. Errors on curve B include all systematic errors. An extreme assumption about the hadronic contribution to the single-γ spectrum would be to ascribe all the excess photon yield at the lowest p_T value (0.9 GeV/c) to this source and if one subtracts this off using the same p_T dependence as the π^0 or η^0 curve C results.

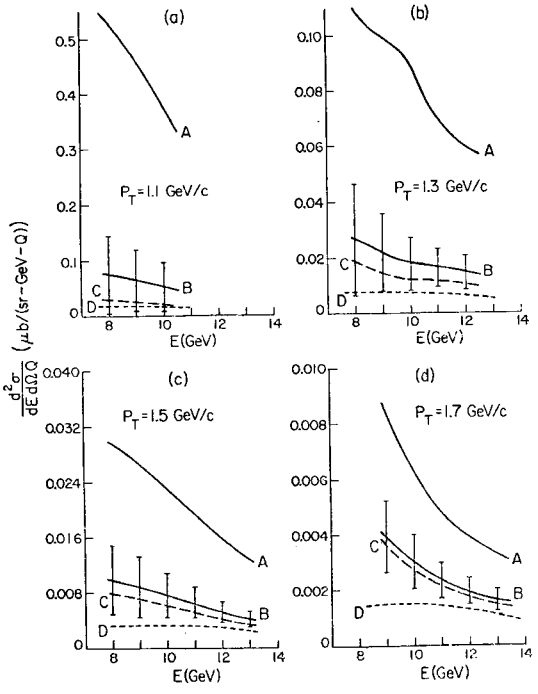

Fig. 2 γ yield at four values of p_T.
Curve A : Single γ yield. Curve B : Single γ yield after subtracting contributions from $\pi^0 \to 2\gamma$, $\eta^0 \to 2\gamma$. Curve C : Single γ yield if all excess at lowest p_T is ascribed to hadronic decay (π^0,η^0) and is subtracted according to p_T dependence of π^0 and η^0 (see text). Curve D : Bjorken-Paschos prediction for integrally charged partons.

The results can be compared with the relation of Bjorken and Paschos[5] by which the parton charge, Q, could in principle be determined independent of details of the parton model from the ratio of inelastic Compton scattering to inelastic electron scattering:

$$\left(\frac{d\sigma}{d\Omega dE}\right)_{\gamma p} \quad \frac{(E_o-E)^2}{E_o E}\frac{\langle \sum_i Q_i^4 \rangle}{\langle \sum_i Q_i^2 \rangle}\left(\frac{d\sigma}{d\Omega dE}\right)_{ep} .$$

Here E_o is the initial and E the final energy of the γ or the e, and $\langle \sum_i Q_i^4 \rangle / \langle \sum_i Q_i^2 \rangle$ must lie between 1/9 and 4/9 for any fractionally-charged quark model. Taking integrally-charged partons, so $\langle \sum_i Q_i^4 \rangle / \langle \sum_i Q_i^2 \rangle = 1$, gives curve D in the figure, well below curve B or even C at high p_T values and having the wrong E and p_T dependence.

This surprising single-photon excess is in qualitative agreement with two earlier experiments.[2,6] One possible explanation is that the sort of interchange model term which fits our π^0 results could be present in inelastic Compton scattering. This $\bar{q}p \to qq\gamma$ subprocess, which actually measures photon rather than proton structure, is consistent with the p_T dependence of the data.

REFERENCES

1. The $\pi^{\pm}$ inclusive yields have recently been reanalyzed by D Sherden.

2. B W Worster, D O Caldwell, V B Elings, B N Kendall, R J Morrison and F V Murphy, Nuovo Cim. Lett. 5(1972) 261.

3. R Blankenbecler and S J Brodsky, SLAC-PUB-1430 (May, 1974) and references contained therein.

4. D C Fries, notes for a seminar at Dubna (Oct. 1972), and private communication.

5. J D Bjorken and E A Paschos, Phys. Rev. 185(1969) 1975.

6. J F Davis, S Hayes, R Imlay, P C Stein, and P J Wanderer, Phys. Rev. Lett. 29(1972)1356.

COMPARISON OF $e^+ - e^-$ DEEP INELASTIC SCATTERING AND WIDE-ANGLE BREMSSTRAHLUNG

D O Caldwell, J P Cumalat, A M Eisner, D L Fancher, T P McPharlin, R J Morrison, F V Murphy, T B Risser and S J Yellin

University of California, Santa Barbara*

Brodsky, Gunion, and Jaffe[1] have suggested that a measurement of $(e^+ + p \to e^+ + \gamma + \ldots) - (e^- + p \to e^- + \gamma + \ldots)$ in the scaling region should provide a strong test of the parton model, and if the model proves valid, a definitive test of whether the constituents of the proton have fractional versus integral charge. This interference between Bethe-Heitler and virtual Compton amplitudes can be expressed in terms of a structure function which, according to the parton model, should depend on only one of the six kinematic variables available. Integration over that variable gives a sum rule involving the charges of the partons. This means of charge determination is on firmer theoretical ground than is that from the inelastic Compton result, and the constituent-interchange term which may contribute so much to the observed single-photon excess cannot enter into the e^+-e^- difference. Furthermore, any spurious hadronic effects, such as the photon decay of some heavy meson, also cannot contribute to the difference.

In addition to an 88-counter photon detector similar to that described above, this experiment had a scattered electron detector which determined the energy, momentum, and angle of the e^+ or e^- which scattered from a hydrogen target when a 13.5-GeV e^+ or e^- beam was incident. The procedure for calibrating, mapping, and maintaining the calibration of the electron energy detector, a hodoscoped Pb-scintillator sandwich, was also similar to that for the photon detector previously described. Our kinematic range covered virtual photon masses of $|q^2|$=1 to 3$(\mathrm{GeV/c})^2$ and energies of ν =2 to 10 GeV.

To reduce systematic errors in the e^+-e^- differences, the beams were made as much alike as possible, and about equal amounts of interleaved e^+ and the e^- data collected at three different beam intensities (3×10^7, 5×10^7, and 7×10^7 e's/pulse). No rate dependence was found, eliminating this possible systematic error.

Analysis of the results is now in progress, and at present we can say only that a difference of the order of 10% seems to be observed, although it is conceivable that future corrections could change this appreciably.

This experiment also measures the difference between the total e^+ and e^- cross sections, which might be expected to be of the order of α from the interference of one- and two-photon exchange. Our preliminary result, integrated over q^2 and ν is $(e^+ - e^-)/(e^+ + e^-) = 0.0025 \pm 0.0016$, with most of the difference at high ν and $1.5 < |q^2| < 2$. The error includes statistical uncertainties in the e^+ and e^- data, the empty target subtraction (actually the same for e^+ and e^-), and the correction for pion contamination. The last effect was measured by reversing the polarity of the recoil-electron analyzing magnet. Because there were more π^+ than π^-, this effect gave a correction of -0.0051 ± 0.0003 to the difference. This result is consistent with that of an alternative method in which Pb was placed in front of the electron detector to attenuate the $e^\pm$ contribution. Note that systematic errors are not included in the result and

*Supported in part by the US Atomic Energy Commission.

that no radiative corrections have been made, as indeed they should not be for some comparisons with theory.

Fishbane and Kingsley[2] have pointed out that if the nucleon has point-like constituents, the e^+-e^- difference could be $\alpha \ln^2(-q^2/\mu^2)$ instead of α. Pati and Salam[3] predict an e^+-e^- difference if a new class of short-range lepton-hadron interactions explain $\sigma(e^+e^- \to \text{hadrons})$. No support for either of these ideas is provided by the unexpectedly small result we get.

REFERENCES

1. S J Brodsky, J F Gunion, and R L Jaffe, Phys. Rev. D6(1972)2487.
2. P M Fishbane and R L Kingsley, Phys. Rev. D8(1973) 3074.
3. J C Pati and A Salam, Phys. Rev. Lett. 32(1974)1083.

COMMENTS ON GENERALIZED VECTOR DOMINANCE

D Schildknecht

DESY

As is well known, about ten years of photon hadron physics for $q^2 \approx 0$ (q^2 = photon four momentum squared) in the multi GeV energy range may be summarized by stating that photons behave hadron-like: indeed, the total photoabsorption cross section from nucleons and complex nuclei, as well as inclusive and exclusive photon induced reactions may be qualitatively and semiquantitatively understood[1] on the basis of hadronlike behaviour as formulated within the framework of ρ^o,ω,ϕ dominance.

It seems thus a fundamental question whether the concepts of hadronlike behaviour and vector dominance remain relevant and useful in the region of large spacelike $q^2 \gtrsim 1$ GeV^2 explored in deep inelastic electron scattering. Some insight into the role of vector mesons in the scaling region may be obtained by quantitatively analysing the ρ^o induced part of the cross section for moderately large $q^2 \cong 1$ GeV^2, where nevertheless scaling sets in precociously. The ρ^o induced part of the transverse photon absorption cross section σ_T is given by

$$\sigma_T^{\rho^o\text{induced}}(W,q^2) = \frac{1}{(1+\frac{q^2}{m_\rho^2})^2} \frac{\alpha\pi}{\gamma_\rho^2} \sigma_{\rho^o p}$$

$$= \frac{16\pi}{\sigma_{\rho^o p}} \frac{d\sigma^{t=o}}{dt} (\gamma_{\text{virt.}} p \to \rho^o p). \quad (1)$$

The fall-off with q^2 according to the ρ^o pole squared is supported by ρ^o electroproduction[2]. The role of ρ^o,ω,ϕ in deep inelastic scattering is best seen by looking[3] at $\nu W_2(\omega',q^2)$ at fixed $\omega' \equiv \frac{W^2}{q^2} + 1$ as a function of q^2 in the large ω' region, where vector dominance considerations are most likely to be relevant. The data on Fig. 1 nicely show the precocious onset of scaling, which goes away completely, however, as soon as the ρ^o,ω,ϕ induced parts are subtracted. The lesson learned from this simple exercise is that vector mesons form an integral part of the scaling phenomenon. This may suggest building up the virtual forward Compton amplitude in terms of vector state forward scattering including all 1^- states produced in e^+e^- annihilation, thus naturally leading to Generalized Vector Dominance (GVD). Moreover, if alternatively unobservable pointlike constituents are introduced to explain scaling, these should apparently be viewed as being dual to observable hadronic vector states.

Having thus hopefully convinced the audience of the

relevance of vector mesons even in the scaling region, let me come to GVD. The q^2 dependence of the virtual photon absorption cross section from nucleons is viewed as being due to the propagation of hadronic vector states, i.e. we have for the transverse part

$$\sigma_T(W,q^2) = \int \frac{m^2\tilde{\rho}(W,m^2,m'^2)m'^2}{(q^2+m^2)\ (q^2+m'^2)}\ dm^2dm'^2 \qquad (2)$$

The spectral weight function $\tilde{\rho}$ contains the vector state photon couplings from e^+e^- annihilation multiplied by vector meson forward scattering amplitudes. Quantitatively successful models[5,6] have been based on the diagonal approximation, $\tilde{\rho} = \rho(W,m^2)\ \delta(m^2-m'^2)$, in which ρ is given by the product

$$\rho(W,m^2) = \frac{1}{4\pi^2\alpha}\ \sigma_{(e^+e^-)}(m^2)\ \sigma_{Vp}(W,m^2). \qquad (3)$$

$\sigma_{e^+e^-}(m^2)$ denotes the $e^+e^-\to$hadrons cross section and σ_{Vp} the total absorption cross section for a hadronic vector state of mass m. The diagonal approximation became increasingly problematic, however, as progressively higher energy data on e^+e^- annihilation became available during the last two and a half years. Let me first discuss these problems and then briefly describe a recent attempt to formulate a model within the off-diagonal framework.

Indeed, with $\rho\sim 1/m^4$ as required for scaling of W_1 and the transverse part of νW_2, and with $\sigma_{e^+e^-}(m^2)\sim 1/m^2$ the vector state absorption cross section σ_{Vp} would have to fall as $1/m^2$ as with a mass independent σ_{Vp} logarithmic divergences and linear violations of scaling are encountered. (Things become even more problematic with $\sigma_{e^+e^-}\sim$ const as indicated by the CEA[7] and SPEAR[8] data beyond about 3.5 GeV c.m. energy). $\sigma_{Vp}\sim 1/m^2$ may be intuitively unsatisfactory and more importantly makes the validity of the diagonal approximation doubtful. Validity of the diagonal approximation with decreasing diagonal terms would require[9] $d\sigma/dm^2 < 1/m^6$ for diffraction dissociation e.g. $\rho_o p \to \rho(m)p$, and it is hard to see how projecting out the spin conserving part should reduce the empirical diffraction dissociation cross section $d\sigma/dm^2 \sim 1/m^2$ as measured for $\pi p \to Xp$ to such a tiny fraction. Furthermore, with $\sigma_{Vp}\sim 1/m^2$ the ρ'' (1600) photoproduction cross section should be much smaller[9] than experimentally observed.

Thus it seems natural and almost compelling to give up the diagonal form and the $\sigma_{Vp}\sim 1/m^2$ law which it engenders and formulate GVD within an off-diagonal framework, although admittedly more freedom is thus

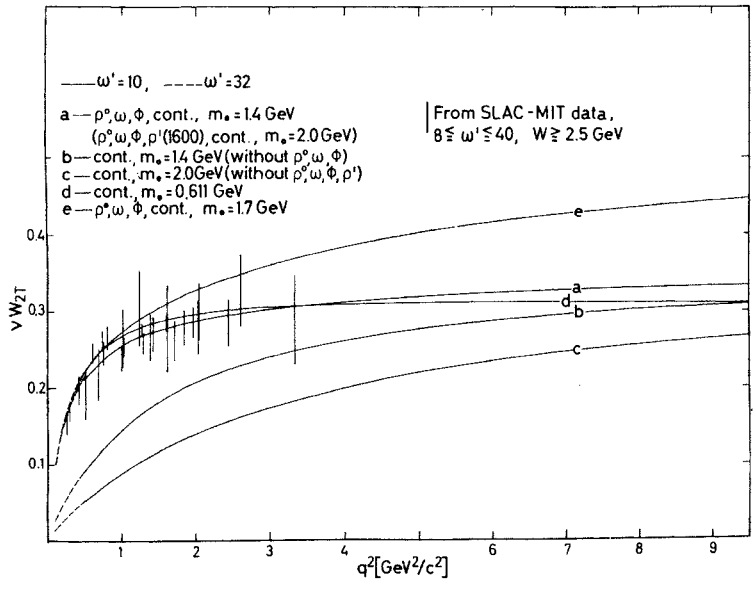

Fig.1 The transverse part of the proton structure function as a function of q^2 for fixed ω' (from ref. 3). For the purposes of the discussion given here curves (a) and (b) only are important, (a) as a fit to the data[4] and (b) showing the result of the ρ^o,ω,ϕ subtraction from curve (a).

introduced into the model. Off-diagonal terms in the Compton forward amplitude correspond to interference between different ingoing vector mesons in the total photon absorption cross section σ_T, which interference may be destructive thus allowing for $\sigma_{e^+e^-} \sim 1/s$, while keeping $\sigma_{Vp} = \text{const.}$ A quantitatively successful model along these lines has been constructed by Fraas, Read and myself[9]. I will briefly describe it next.

Mainly for technical reasons the model has been formulated with a discrete spectrum of vector mesons $V_N (N=0,1,\ldots)$ choosing vector meson photon couplings such that $\sigma_{e^+e^-} \sim 1/s$ is reproduced consistent with data up to 3.5 GeV c.m. energy (Fig. 2). Moreover, negative phases are introduced by assuming $1/\gamma_N \sim (-1)^N$ for the vector meson photon couplings, motivated from negative contributions needed for the nucleon form factors and also obtained in quark model calculations[10]. As for the hadron physics, $\sigma_{\rho_N p} = \sigma_{\rho_o p}$ independent of N is assumed, and diffraction dissociation amplitudes are introduced by a power law taking into account effective transitions to next neighbors only. Convergence of $\sigma_T (W, q^2 = 0) \equiv \sigma_{\gamma p}(W)$ and normalization to the observed magnitude of $\sigma_{\gamma p}$ fixes the constants in the off-diagonal diffraction dissociation type terms. The q^2 dependence is then predicted to be ($\omega' \gtrsim 8$)

$$\sigma_T(W, q^2) = \frac{\bar{m}^2}{(q^2+\bar{m}^2)} \sigma_{\gamma p}(W), \qquad (4)$$

where $\bar{m}$ is obtained to be somewhat smaller than the ρ^o mass, $\bar{m}^2 = 0.61\, m_\rho^2 = 0.36$ GeV^2. It is amusing to note that the same formula (4) motivated from a different reasoning had previously been shown[3] to fit the data with $\bar{m}^2$ fitted to be 0.37 GeV^2 in good agreement with the value now calculated. Thus we expect good agreement with the data as demonstrated for σ_T in Fig. 3 and for the precocious approach to scaling of the transverse part of νW_2 in Fig. 4. Formula (4) also implies[1] $\omega_W \equiv (2M\nu + b^2)/(q^2 + a^2)$[11] to be a good scaling variable, provided $a^2 \equiv \bar{m}^2$, and a^2 had indeed been obtained from fits[12] to be $a^2 \gtrsim 0.38$ to 0.42 GeV^2. Let me add two comments on these results. First of all, from $\sigma_{e^+e^-}$ approximatley constant as recently observed beyond 3.5 GeV, one would expect positive violations of scaling in νW_2 for large ω', and sufficiently large q^2 where scaling has not been very well tested. Indications for positive violations of scaling for large ω are indicated by the NAL μ experiment as reported by Hand[13] to this conference.

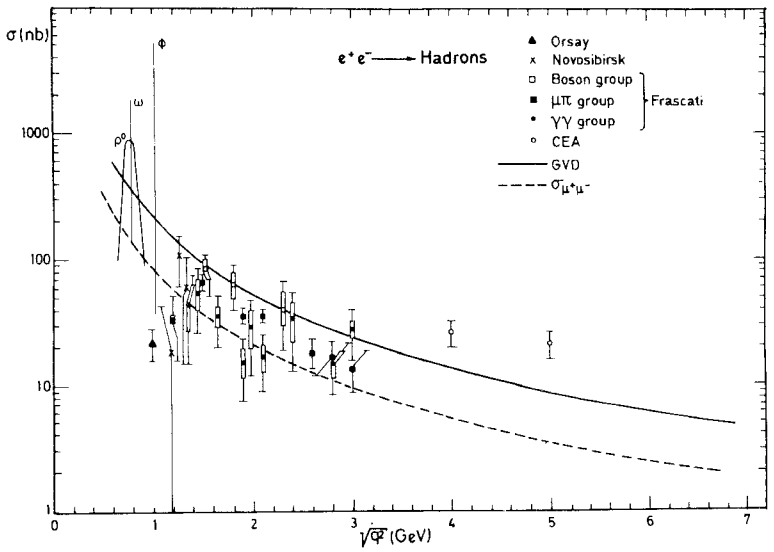

Fig. 2 The e^+e^- annihilation cross section with the GVD curve used to predict deep inelastic ep scattering (ref. 9).

Secondly, concerning $R \equiv \sigma_L/\sigma_T$, let me remind you of the GVD prediction[5] $R \sim \xi \ln(q^2/m_\rho^2)$ (for q^2, W^2 large, $\omega' \gtrsim 10$) with $\xi \equiv \sigma_{\rho^o p}^{\text{long.}}/\sigma_{\rho^o p}^{\text{transv.}}$ which prediction is also valid in the off-diagonal framework. It is of great interest in this connection that larger values of R than the previously reported average of $R \cong 0.18$ seem not to be excluded by the data[14] anymore, especially for large values of $\omega' \gtrsim 10$. The influence of off-diagonal transitions has also been investigated[15] for ρ^o electroproduction. Although changes for t = 0 relative to simple ρ^o dominance are small, off-diagonal terms may be responsible for possible changes of the ρ^o slope with increasing q^2. We conjecture that a possible flattening of the ρ^o slope with q^2 ("photon shrinkage") is related to observed differences in slope between elastic hadron hadron scattering and diffraction dissociation. For details I have to refer to ref. 15, but I would like to show a quantitative result on fig. 5.

Finally let me add a remark on shadowing in complex nuclei. Fig. 6 shows the result of a recent DESY experiment[16] contributed to this conference, in which the existence of shadowing has been shown for the first time for forward Compton scattering. The situation is less clear for $q^2 > 0$ as investigated in inelastic electron scattering. As ρ^o meson electro-production has been observed for $q^2 > 0$, we expect shadowing as quantitatively[17] shown on Fig. 7. Unfortunately data with small errorbars are available at rather low energies only, where the effects to be expected are small. New data from NINA (fig. 8) do not show shadowing for $q^2 > 0$. The theoretical expectations of Fig. 7 could be changed, if rapid phase changes occur with increasing q^2 or if ρ^o electroproduction would fall off considerably faster than expected from ρ^o dominance. Anyway, further data on inelastic electron scattering from complex nuclei for small q^2 but at high energies ($\gtrsim$ 15 GeV) would certainly help to clarify the situation.

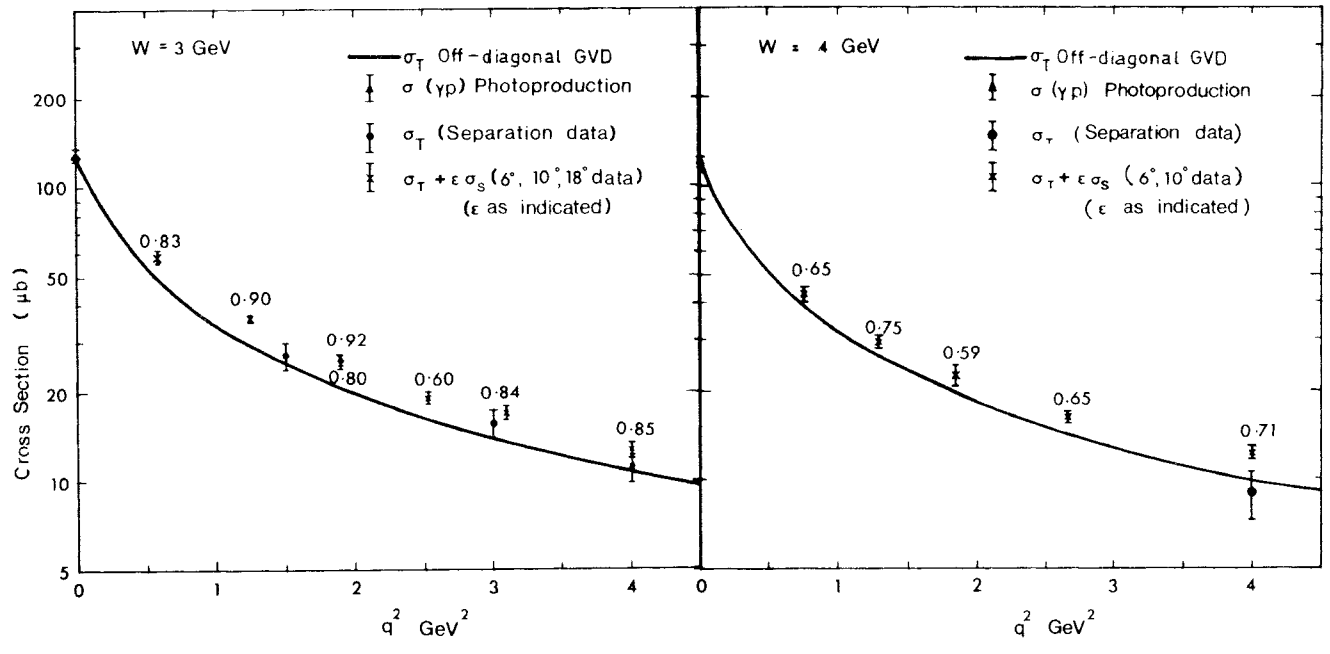

Fig.3 Off-diagonal GVD prediction from (4) for $\sigma_T(W,q^2)$ as a function of q^2 (ref. 9) compared with SLAC-MIT data[4].

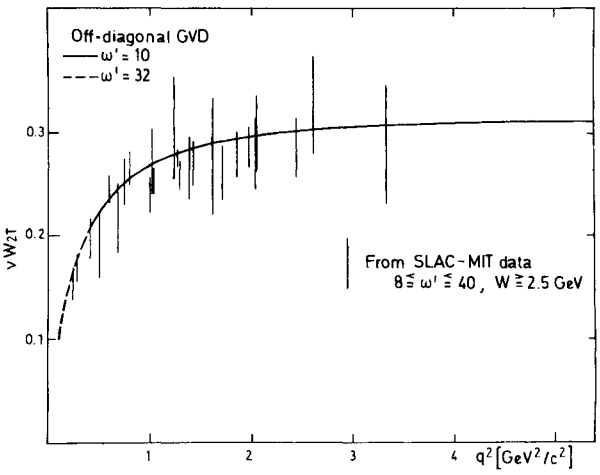

Fig.4 The transverse part of the proton structure function νW_2 as a function of q^2 in the large ω' diffraction region showing the precocious approach to the scaling limit (compare ref. 9 for details).

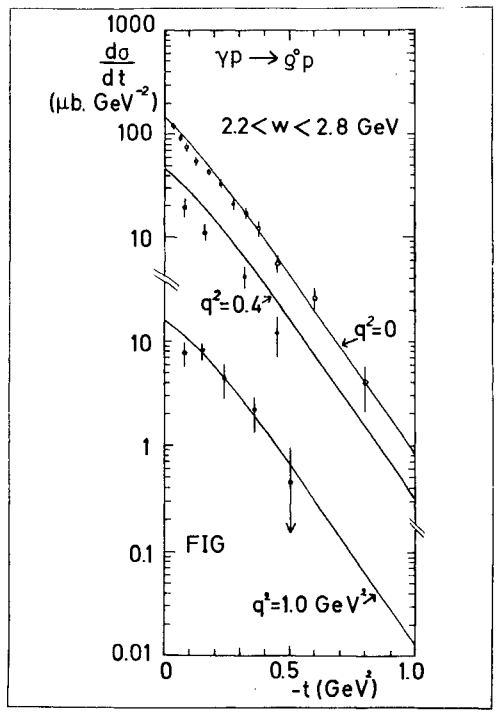

Fig. 5 The t dependence of the differential cross-section for rho photo- and electroproduction, showing how the inclusion of higher vector mesons can flatten the slope - especially for small $|t|$ and large q^2. (DESY-data[2] points and SBT photoproduction, see ref. 15 for details).

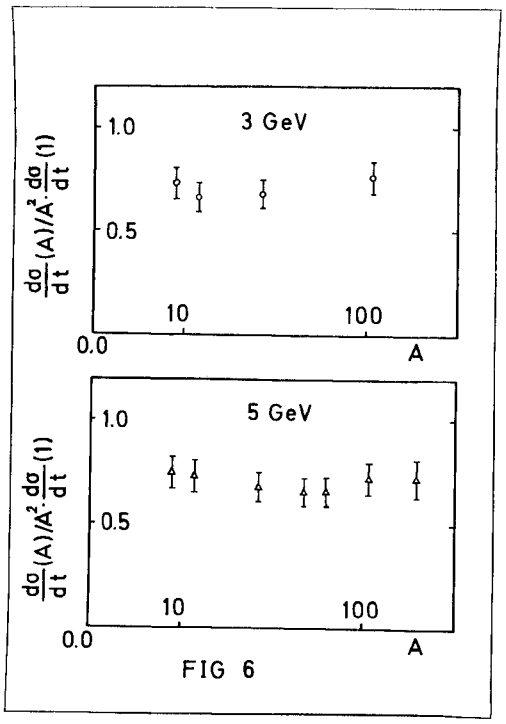

Fig.6: Shadowing in Compton scattering (ref. 16) as observed at DESY.

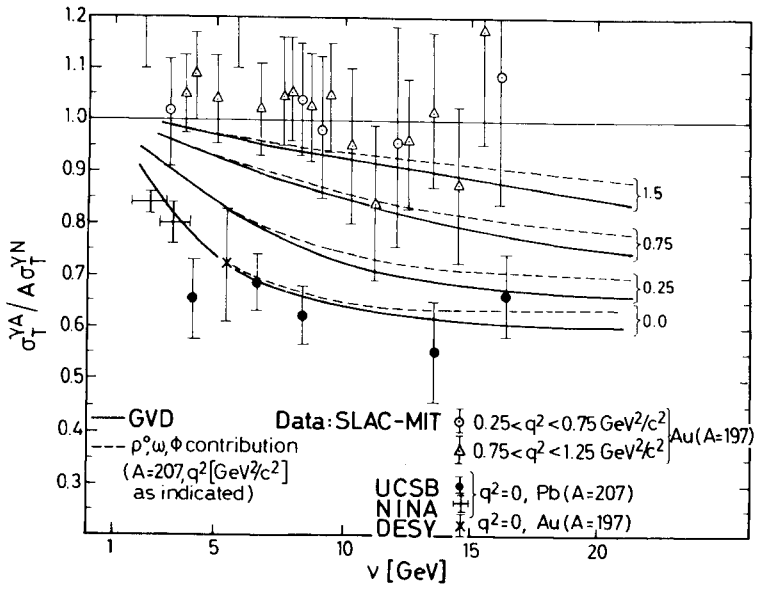

Fig.7 Shadowing for photoproduction and inelastic electron scattering (from ref. 17).

In conclusion, let me collect some of the main points which have been made:

1. The low lying vector mesons ρ^0,ω,ϕ form an integral part of the scaling phenomenon. Without the ρ^0,ω,ϕ induced contribution scaling is no longer precocious.

2. Off-diagonal GVD allows for $\sigma_{e^+e^-} \sim 1/s$ together with reasonable hadron physics. Precocity of scaling naturally follows from the smallness of the mass parameter, which sets the scale and is computed to be $\bar{m}^2 = 0.61 m_\rho^2$. $\sigma_{e^+e^-} \sim$const creates problems and may lead to positive scaling violations for large ω', for q^2 sufficiently large.

3. Off-diagonal transitions can explain possible "photon shrinkage" effects in vectormeson electroproduction.

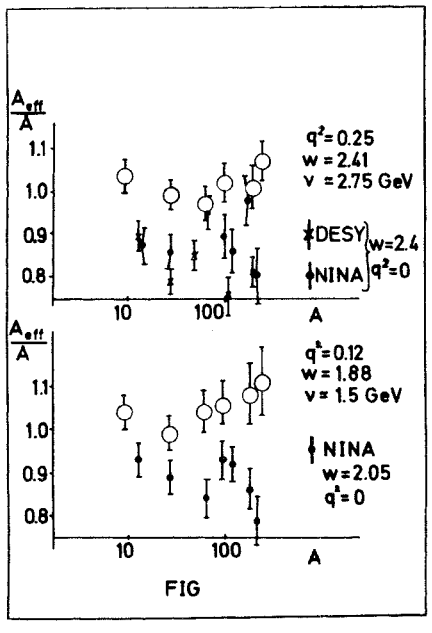

Fig.8 Photoproduction and inelastic electron scattering as measured at NINA (ref. 18).

4. Further search for higher mass vector mesons, comparison of $e^+e^- \to$ hadrons with diffractive photo- and electroproduction in the 100 GeV energy range and more data on large ω' deep inelastic scattering are important to provide further tests of GVD in the near future.

REFERENCES

1. e.g. J.J. Sakurai, Erice Lectures 1971 and 1973. D. Schildknecht, Springer Tracts in Modern Physics, Vol. 63, p. 57 (1972).
2. e.g. V. Eckardt et al., DESY 74/5 (1974).
3. B. Gorczyca and D. Schildknecht, Phys. Letters 47B, 71 (1973).
4. E.D. Bloom et al., Phys. Rev. Letters 23, 930 (1969) G. Miller et al., Phys. Rev. 5, 528 (1972).
5. J.J. Sakurai and D. Schildknecht, Phys. Letters 40B, 121 (1972); 41B, 489 (1972); 42B, 216 (1972) and J.J. Sakurai, Proc. of the 1972 McGill University Summer School, p. 435; D. Schildknecht, Proc. of the Eighth Rencontre de Moroind ed. by J. Tran Thanh Van, Vol. 1, p. 181 (1973).
6. A. Bramon, E. Etim and M. Greco, Nucl. Phys. B63, 398 (1973); M. Greco, Nucl. Physics B63, 398 (1973).
7. K. Strauch, Proc. of the Int. Symp. on Electron and Photon Interactions at High Energies, Bonn 1973.
8. B. Richter, this conference.
9. H. Fraas, B. Read and D. Schildknecht, DESY 74/23, contr. 550.
10. M. Böhm, H. Joos and M. Krammer, Acta Physica Austriaca 38, 123 (1973).
11. V. Rittenberg and R.H. Rubinstein, Phys. Lett. 35B, 50 (1971).
12. F.W. Brasse et al., Nucl. Phys. B39, 521 (1972).
13. D.J. Fox et al., CLNS-273 (1974), contribution 330.
14. E.M. Riordan et al., SLAC-PUB-1417, contribution 762.
15. H. Fraas, B. Read and D. Schildknecht, contribution 551, Daresbury report in preparation.
16. L. Criegee et al., Contribution to this conference.
17. D. Schildknecht, Nucl. Phys. B66, 398 (1973).
18. J. Bailey et al., Contribution to this conference.

INCLUSIVE DEEP INELASTIC LEPTO PRODUCTION

R Cahn

University of Washington, Seattle

The most comprehensive predictions for $\gamma^* p \to hX$ and $W^{\pm} p \to hX$ come from the quark-parton model of Feynman[1] and Bjorken and co-workers[2]. The phase space for the final state depends only on $s = W^2 = M^2 + 2M\nu - Q^2$, where p is the target momentum, q is the photon (or W) momentum and where

$$\begin{aligned} M\nu &= p.q \\ Q^2 &= -q^2 \ . \end{aligned} \qquad (1)$$

The rapidity distribution has a length $Y \cong \log s/M^2$ (if the transverse momentum of h is limited).

For $\omega = 2M\nu/Q^2$ large (the Regge region) there are five[3,4] domains: I. target fragmentation (length ~2 in rapidity), II. hadronic plateau (length ~log (w-1)), III. hole fragmentation (length ~2), IV current plateau (length ~log Q^2/M^2), and V. parton fragmentation (length ~2). See Fig.1.

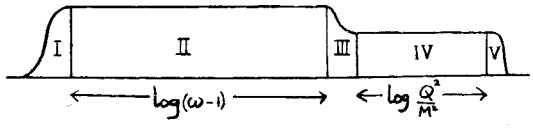

Fig.1

Regions I and II are anticipated to be identical with those found in hadron-hadron collisions. Regions V and IV are anticipated to be identical with those predicted[1,2] by the parton model for $e^+e^- \to hX$. Data from CEA[5] and SPEAR[6] indicate a grave failure of the quark-parton model which we shall remark upon below. Region III is unique to deep inelastic leptoproduction. A simple prediction of this model is that for multiplicities[4]:

$$\langle n \rangle_{\substack{ep \\ \nu p}} = C_{had} \log(\omega - 1) + C_{e^+e^-} \log(Q^2/M^2) + \text{const}$$

where hadronic multiplicites are given by $\langle n \rangle_{had} = C_{had} \log s + \text{const}$ and e^+e^- multiplicities are given by $\langle n \rangle_{e^+e^-} = C_{e^+e^-} \log(Q^2/M^2) + \text{const}$. Data so far indicate similar coefficients for $\log(\omega - 1)$ and $\log Q^2$[7].

For the parton fragmentation region (V) more precise predictions can be made[8]. The appropriate longitudinal variable in this region is $z = \frac{-2p' \cdot q}{Q^2}$ where p' is the four-momentum of the observed hadron. In the Breit frame of the virtual photon and the struck parton, z is the fraction of the struck parton momentum present in the observed hadron. The inclusive spectrum (ω fixed, integrated over $p_\perp$) is given by[8]

$$\frac{1}{\sigma} \frac{d\sigma}{dz} = \frac{\sum_i \sigma_i(x) D_i^h(z)}{\sum_i \sigma_i(x)} \qquad (1)$$

where $\sigma_i(x)$ is the contribution of quark-type i to the γ^* or W cross section at $\omega = 1/x$. For example, for $\gamma^* p$, $\sigma_u \propto \frac{4}{9} u(x)$, $\sigma_d \propto \frac{1}{9} d(x)$. For $x > 0.2$ there are few anti-quarks or strange quarks. The functions $D_i^h(z)$ represent the density of hadrons of type h arising from quark-type i and carrying a fraction z of the quark momentum. If we let $\eta(z) = D_u^{\pi^+}(z)/D_d^{\pi^+}(z)$ and $r(x) = u(x)/d(x)$ we have

$$\frac{\frac{d\sigma}{dz}_{\gamma^* p \to \pi^+ X}}{\frac{d\sigma}{dz}_{\gamma^* p \to \pi^- X}} = \frac{r(x)\eta(z) + 1/4}{r(x) + \eta(z)/4} \ , \qquad (2)$$

assuming only u and d quarks present ($x \gtrsim 0.2$).

Similarly we have

$$\frac{\frac{d\sigma}{dz}_{\gamma^* n \to \pi^+ X}}{\frac{d\sigma}{dz}_{\gamma^* n \to \pi^- X}} = \frac{\eta(z) + r(x)/4}{1 + r(x)\eta(z)/4} \quad . \qquad (3)$$

In the same approximation

$$\frac{\sigma_{\gamma^* p}}{\sigma_{\gamma^* n}} = \frac{r(x) + 1/4}{1 + r(x)/4} \quad . \qquad (4)$$

Thus $r(x) > 1$ since $\sigma_{\gamma^* p}/\sigma_{\gamma^* n} \simeq 1 - \frac{3}{4}x$.

These predictions are borne out reasonably well by the data. The value of η has been estimated[10] to be about 3 for $0.4 < z < 0.8$, but, for $z \ll 1$, η should tend to unity while it should be quite large for $z \simeq 1$. The difference between $\gamma^* n \to pX$ and $\gamma^* p \to pX$ is slight[11] as might have been anticipated since $\eta'(z) = D_u^p(z)/D_d^p(z)$ should be nearer unity than is $\eta(z)$.

The hole fragmentation region has not been explored experimentally. The requirements of large Q^2 and ω dictate NAL parameters at least. The features of this region can be determined if the data are considered as a function of $y' = y_{lab} - \log(\omega - 1)$ or as a function of $z = \frac{-2p'.q}{Q^2}$.

Despite the apparent adequacy of the quark-parton model for inclusive leptoproduction, its failure in e^+e^- annihilation casts grave doubts on its reliability. It may well be, however, that suitably normalized quantities, e.g. $\frac{1}{\sigma}\frac{d\sigma}{dz}$ will be reasonably predicted by the model. In fact many of the predictions rely mostly on the internal quantum numbers of hadronic constituents rather than their dynamics.[12]

An attempt to confront the breakdown of scaling has been made by Stack[13] who relates the breakdown to the inclusive distribution. Defining $\gamma(n)$ by

$$\int_1^\infty \frac{F(\omega, Q^2)}{\omega^n} d\omega \propto (Q^2)^{-\frac{1}{2}\gamma(n)} \quad , \qquad (5)$$

he categorizes theories by

class I: $\gamma(n) \to$ const. as $n \to \infty$,

class II: $\gamma(n) \to \infty$ as $n \to \infty$.

Bjorken scaling requires $\gamma(n) = 0$. Since no known field theory gives Bjorken scaling and since other class I theories appear to have jets of high transverse momentum particles which have never been observed, Stack concludes class II theories are favoured. This class includes the asymptotically free field theories.

If one seeks only a phenomenological description recourse to elaborate theories is unnecessary. In contrast with inclusive e^+e^- annihilation data[6], deep inelastic leptoproduction data available at present are not in conflict with the naive quark-parton model.

REFERENCES

1. R.P. Feynman, Phys.Rev.Lett. 23, 1415(1969); and in High Energy Collisions (Gordon & Breach, New York, 1969), p.237.
2. See, for example, S.M. Berman, J.D. Bjorken, and J.B. Kogut, Phys.Rev. D4, 3388 (1971).
3. J.D. Bjorken, Phys.Rev. D7, 282 (1973).
4. R.N. Cahn, J.W. Cleymans, and E.W. Colglazier, Phys.Lett. 43B, 323 (1973). R.N. Cahn & E.W. Colglazier, Phys. Rev. D8, 3019 (1973).
5. A. Litke et al. Phys.Rev.Lett. 30, 1189 (1973) G. Tarnopolsky et al. Phys.Rev.Lett. 32, 432 (1974).
6. See B. Richter's talk at this conference.
7. P.H. Garbincius, et al. Phys.Rev.Lett.32, 328(1974). A.J. Sadoff, et al. Phys.Rev.Lett. 32, 955(1974). V. Eckardt et al., Paper 392.
8. S.D. Drell and T.-M. Yan, Phys.Rev.Lett.24, 855(1970). M. Gronau, F. Ravndal, Y. Zarmi, Nuc.Phys. B51, 611 (1973) R.P. Feynman, Photon-Hadron Interactions (Benjamin, 1972).

9. C.J. Bebek, et al. Paper 572.
J.T. Dakin, et al. Paper 160

10. J.T. Dakin and G.J. Feldman, Phys.Rev. D8, 2862 (1973). J. Cleymans and R. Rodenberg, Phys. Rev. D9 155 (1974).

11. C.J. Bebek, et al. Paper 573.

12. F. Close, private communication.

13. J. Stack, Paper 397.

SCALING IN PARTON MODELS

J C Polkinghorne

DAMTP University of Cambridge

We may not yet be seeing scale breaking in deep inelastic electroproduction - the situation appears to be less alarming than rumour had seemed to suggest. (Of course in e^+e^- the situation is baffling, but perhaps the time-like region is more complicated anyhow.) However doubtless one day we shall see it. It would be truly remarkable if it had been given to our generation to discover the absolutely fundamental constituents of matter! Thus if partons now appear pointlike there will doubtless come a regime in which they have a discernable size. The effect of this is rather simple to think about. As Drell and Chanowitz[1] pointed out the point like current coupling will be changed in a way represented by the substitution

$$1 \to \frac{1}{1 - q^2/\Lambda^2} \simeq 1 + q^2/\Lambda^2 \qquad q^2 \ll \Lambda^2 \tag{1}$$

This naive picture produces effects of opposite sign and corresponding magnitude in electroproduction ($q^2 < 0$) and e^+e^- ($q^2 > 0$) but one can arrange for different effects in the two regions if one also gives the partons an anomalous magnetic moment. This was pointed out by West[2] who noted that one could suppose that nature had been so clever (or perverse) as to arrange the parameters so that the effects cancelled out in electroproduction. A similar scheme has been discussed by Matumato and Tojima (156). Such theories, however, give a value of R which increases with q^2.[3]

In field theories with anomalous dimensions one does not get scaling but the moments of the structure functions satisfy relations of the form

$$\int \frac{F_2(\omega, q^2)}{\omega^n} d\omega = C_n \left(\frac{M^2}{-q^2}\right)^{\frac{1}{2}\gamma(n)} \tag{2}$$

Bloom discussed the phenomenological evidence for this at Bonn; it is poor. Stack (397) has pointed out that theories can be classified accordingly as

$$\begin{aligned} &\text{I} : \gamma(n) \to \text{const.}, \quad n \to \infty ; \\ &\text{II} : \gamma(n) \to \infty \quad , \quad n \to \infty . \end{aligned} \tag{3}$$

He finds that type I theories have a sort of generalised "handbag" structure (like parton models) with its suggestion of jet structure, whilst this is not necessarily so in type II theories. This latter class includes asymptotically free theories for which $\gamma = O(g^2 \ln n)$.

It is also interesting to consider the next-to-leading order correction terms in parton models. Canonically these are expected to be of order ν^{-1} but non-canonical behaviour $\nu^{-\varepsilon}$ ($\varepsilon < 1$) is possible, as Osborn and Woo[4] first realised. It is

an interesting result that ε must be less than $\frac{1}{2}$ in "stretched' parton models, that is those which give large final state multiplicities.

The argument[5] is readily illustrated by reference to the handbag diagram, fig.1. We will concentrate on the

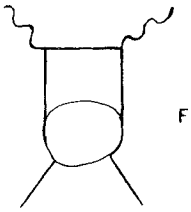

Fig.1

propagator at the top of the diagram (fragmentation of the struck parton) but similar arguments apply to the lower half of the diagram. Consider the propagator at large k^2

$$\int \frac{\rho(m^2)\ dm^2}{k^2-m^2} \sim \frac{1}{k^2} + \int \frac{\rho(m^2)m^2dm^2}{(k^2)^2}+\ldots \qquad (3)$$

The first term gives the scaling result, and we have used the normalization condition

$$\int \rho(m^2)\ dm^2 = 1 \qquad (4)$$

If the integral in the second term is convergent one has the canonical correction. If, however, it is divergent then the expansion (3) does not give the correct asymptotic behaviour. A more careful assessment then shows that if

$$\int^{\Lambda^2} \rho(m^2)\ m^2dm^2 \sim (\Lambda^2)^{1-\varepsilon}, \quad \Lambda^2 \to \infty \qquad (5)$$

then the next-to-leading term in the propogator behaves like

$$\frac{1}{(k^2)^{1+\varepsilon}} \qquad (6)$$

giving the non-canonical correction referred to.

Now $\rho(m^2)$ is the weight of intermediate states of mass m in the propagator. If these states give multiplicity $\bar{n}(m^2)$ then the average multiplicity from the struck parton fragmentation is given by

$$< n > = \int \rho(m^2)\ \bar{n}(m^2)dm^2 \qquad (7)$$

For increasing multiplicities this must diverge. Since $\bar{n}(m^2) \sim m$ at most this means that

$$\rho(m^2) \sim \frac{1}{(m^2)^{1+\varepsilon}}, \quad \varepsilon < \tfrac{1}{2}, \qquad (8)$$

which from (5) and (6) leads to the conclusion stated earlier, that if multiplicities are large the corrections to scaling cannot decrease faster than $\nu^{-\frac{1}{2}}$.

Finally one can consider the ω dependence of these terms. If one writes

$$\nu W_2 = F_2(\omega) + \nu^{-\varepsilon} \tilde{F}_2(\omega), \qquad (9)$$

then one knows that

$$F_2(\omega) \sim \text{const.} \qquad \omega \to \infty, \qquad (10)$$

and one can show[5]

$$\tilde{F}_2(\omega) \sim \omega^{\varepsilon}, \quad \omega \to \infty, \qquad (11)$$

so that these effects are likely to be most important at large ω.

REFERENCES

1. M S Chanowitz and S D Drell, Phys. Rev. D9(1974)207?
2. G B West, Phys. Rev. D10(1974)329.
3. F E Close, Daresbury Preprint, DNPL/P154 (1972) unpublished.
4. H Osborn and G Woo, Nucl. Phys. B62(1973)413.
5. R L Kingsley, P V Landshoff, C Nash and J C Polkinghorne, Nucl. Phys. B65(1973)397.
6. C P Jackson, DAMTP preprint in preparation.

LEPTON PHYSICS AND GAUGE THEORIES[+]

A De Rújula

Harvard University, Cambridge, Massachusetts

I am supposed to review the progress in the following topics:

Gauge theories of the weak and electromagnetic interactions and lepton physics (inclusive and exclusive neutral currents, heavy leptons, intermediate vector bosons, deviations from Cabibbo's phenomenology, charm, violations of charge symmetry and the isospin rules, prompt dimuons, strange behaviour of the strange particle production etc.) and gauge theories of the strong interactions and the breakdown of scaling in electron and neutrino scattering.

Having only fifteen minutes I will reluctantly drop the subject of neutral currents and concentrate on the rest.

I. Inclusive Neutrino Scattering in Unified Gauge Theories

This is a topic on which much has already been said in the past. I am motivated by experiment in bringing it to the fore again. Several (two) very beautiful neutrino induced prompt dimuon events have been reported[(1)]. We have also been presented a very preliminary analysis of ν and $\bar{\nu}$ data that may show rather unconventional features[(2)]. We are advised not to jump to conclusions from this preliminary study but, perhaps, we should be ready.

By now many ears are bent from hearing that to lowest order in charged vector and axial vector weak couplings, the inclusive differential ν ($\bar{\nu}$) cross section on an isoscalar target is:

$$\frac{d\sigma^{(\bar{\nu})}}{dx\,dy} = \frac{G^2 m_p E_\nu}{\pi}\left[(1-y+\frac{y^2}{2})F_2(x) \mp (y-\frac{y^2}{2})xF_3(x) - \frac{y^2}{2}F_L(x)\right]$$

$$x = \frac{Q^2}{2\nu}\,, \quad y = \frac{\nu}{m_p E_\nu} = \frac{E_\nu - E_\mu}{E_\nu} \qquad (1)$$

The notation is conventional. Masses have been neglected relative to neutrino energies. Scaling and charge symmetry have been assumed. Corrections proportional to $\sin^2\theta$ [Cabibbo] have been dropped. If the ν and $\bar{\nu}$ data show large deviations from a simultaneous description by Eq.(1), something interesting is going on and some assumption must be dropped. In the context of gauge theories one finds a considerable wealth of reasons why deviations from Eq.(1) may or should occur. At large Q^2 the intermediate vector boson propogator will produce "trivial" deviations from scaling. Other superbly nontrivial deviations are discussed in the second part of this talk. Charge symmetry is explicity violated by the extra charmed piece in the charged weak current and may be a bad approximation when charmed hadrons are produced (Fig. 1a). We return to this topic later. Heavy leptons (Fig. 1b) or the production of vector bosons in the electromagnetic field of the nucleus (Fig.1c) could mock the local production of muons but would not obey Eq.(1). In principle all these effects may come hand in hand with dimuon events (Figs. 2a,b,c). Other conventional explanations of the dimuon events seem to be excluded. For instance, the four-fermion interaction in the Coulomb field of a nucleus (Fig.3) is $O(Z\alpha)^2$ if coherent, but the observed dimuons come with a highly inelastic hadron shower.

[+]Work supported in part by the NSF under grant No. GP40397X.

Charmed hadrons were invented to explain the suppression of strangeness changing neutral currents relative to the strangeness conserving ones[3]. They fail in doing so if they are too heavy[4]. Heavy leptons or intermediate vector bosons do not come in general with upper limits for their masses. In the case of charmed particles, it is hard to avoid the conclusion that they should be produced at present accelerator energies. The case for their search is good, if only as a way to discredit theoreticians. Neutrinos are exceptional in being able to produce charmed particles singly. This occurs above charm threshold, when the second part of the "complete" Glashow-Iliopoulos-Maiani current acts. In a quark notation:

$$J\left[\text{GIM}\right] = J\left[\text{Cabibbo}\right] + J\left[\Delta C \neq 0\right]$$

$$= \bar{p}(n\cos\theta_c+\lambda\sin\theta_c)_L+\bar{p}'(\lambda\cos\theta_c-n\sin\theta_c)_L \qquad (2)$$

Let W be the invariant mass of the final hadrons:

$$W^2 = -Q^2 + 2\nu + m_p^2 = 2m_pE_\nu y(1-x)+m_p^2$$

and M_c the mass of the lightest charmed state with unit baryon number. If a charmed threshold is crossed as E_ν increases ($2m_pE_\nu > M_c^2-m_p^2$) extra events will pop up between the moving kinematical limits

$$1 > y > \frac{M_c^2-m_p^2}{2m_pE_\nu}$$

$$0 < x < 1 - \frac{M_c^2-m_p^2}{2m_pE_\nu}$$

The best place to look for them may be antineutrinos at high y, where the "conventional" distribution is depleted. The differential $d\sigma/dW$ cross section will show a structure and the total cross section will rise.

It must be stressed that in models with pointlike constituents, the threshold for charm is not like others, say the $K\bar{K}$, $p\bar{p}$ or seventeen pion thresholds. These new channels somehow add up to a dull behaviour called scaling. Above charm threshold, contrarywise, the possibility exists of producing new particles with pointlike strength. When the kinematical threshold effects are over ($m_pE_\nu >> M_c^2$), the strength of the interaction nominally doubles. (See Eq.2). In explicit quark parton models, however, the situation is much less optimistic. If charmed particles are produced on p and n quarks the effect (see Eq.2) is down by $\sin^2\theta_c$. Charm is produced through the $\cos\theta_c$ piece of the current on the λ and $\bar{\lambda}$ quarks, but there may be few of these. The preceding

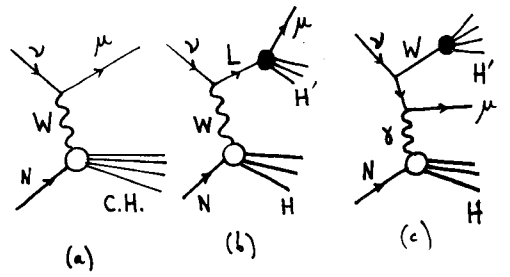

Fig. 1

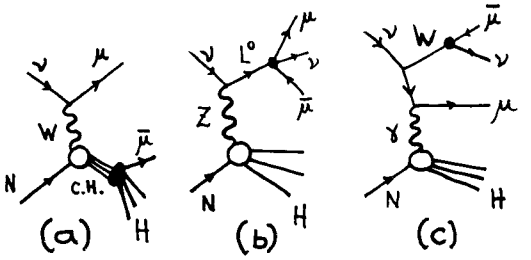

Fig. 2

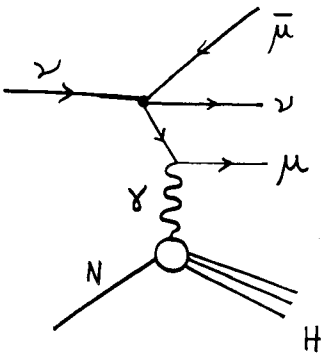

Fig. 3

arguments may not apply to the production of single charmed particles and resonances and the hopes of having an observable effect are not so dim.

Charm may also give rise to interesting exclusive effects (other than dimuon production). Examples are the apparent violation of the $\Delta S = \Delta Q$ rule and a possible apparent increase of associated strange particle production.

CONCLUSION (which I reach at every Conference). The situation will be clear by the time of the next conference.

II. The breakdown of Bjorken scaling in gauge theories of the strong interactions

The following is a respectable opinion: in particle physics, for the statement "We understand..." to be true, it is generally necessary that "..." follow from first principles or from a justifiable perturbation treatment of field theory. I now want to discuss whether "We understand Bjorken scaling" is likely to become true (or proven false) in the near future. I will pretend that the lack of time makes me forget about the timelike region.[5]

We now have renormalizable gauge field theories that are asymptotically free[6]. In these theories the forces between quarks are mediated by vector gluons that interact strongly. Thus, perturbation theory would seem useless. However, when a nucleon is probed by a weak or electromagnetic current at high Q^2, a marvellous hat trick is feasible: the perturbation expansion can be re-expressed in terms of an effective coupling constant $\bar{g}(Q^2)$ that tends to zero as Q^2 increases (see Fig.4). Hence, by construction and demonstration, there are kinematical regimes in which the strong interactions are amenable to a consistent perturbation theory treatment. This is worth repeating: the strong interactions are slowly turned off at high Q^2 and there is hope to "understand" scaling: a free field theory result. Moreover, scaling is predicted not to be exact at any finite Q^2. A very specific pattern of deviations should take place, making the underlying ideas (hopefully) testable.

For the sake of definiteness I will restrict myself in what follows to the model with the twelve "observed" quarks (red, white and blue quartets of p,n,λ and charmed p'). The qualitative and semi-quantitative nature of the results is stable under changes in the model [i.e., the number of quarks or colours] which are not inmoderate.

As Prof. Gross just discussed[7], asymptotically free theories predict the Q^2 dependence of the x-moments of inclusive structure functions (no Q^2 dependence if the theory scaled exactly). These predictions are hard to test but can sometimes be re-expressed as statements on the Q^2 dependence of the structure functions themselves. Given an empirically known structure function $F(x,Q_o^2)$ at a fixed (large) reference momentum Q_o^2, the theory predicts $F(x,Q^2)$ at any other (large) Q^2. The need for so much input stems from our ignorance of the dashed blob in Fig. 4, where the honest to goodness strong dynamics is concealed.

For the theory to apply, it is necessary that m_p^2/Q^2 be small. At present, there is no hope to understand "early" scaling. For the lowest order perturbation calculation to be a good approximation, it is moreover

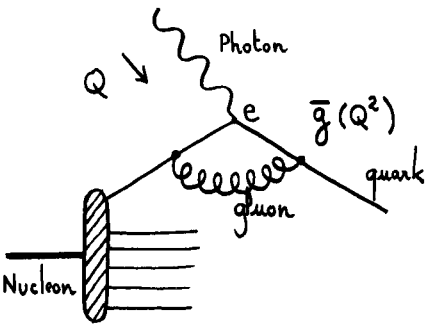

Fig. 4

necessary that the effective expansion parameter be small. In the model under discussion this means $\bar{g}^2/4\pi^2 \simeq 12/(25 \ln Q^2/\Lambda^2)$ small. This is not saying much, since the parameter Λ, that reflects the value of the gluon-quark coupling at a given Q^2, is not predetermined by the model.

The statements in the previous paragraph should be stripped of some propaganda. It is only for suitably chosen structure functions or combinations thereof that just one class of operators contributes to the Wilson expansion and it is enough to know $F(x,Q_o^2)$ at one reference momentum to predict $F(x,Q^2)$. The examples of experimental interest where this is so are:

$F(x,Q^2)$ =
- i) $F_2(ep) - F_2(en)$.
- ii) $F_2(\nu) - F_2(\bar{\nu})$ on any fixed target.
- iii) $xF_3(\nu)$ and $xF_3(\bar{\nu})$ on any target.

A discussion of their relative practical merits and demerits, and more details can be found in the work of elements of the Harvard renormalization group[8], who elaborated on earlier publications.[9]

We lack high Q^2 data. To illustrate the qualitative nature of the predicted scaling violations we must make a guess of an input $F(x,Q_o^2)$. Take

$$F(x,Q_o^2) = x^{\frac{1}{2}}(1-x)^3$$

The $x^{\frac{1}{2}}$ factor is a Regge prejudice, while the $(1-x)^3$ factor is an educated guestimate based on the connection between the structure functions near theshold and the elastic form factors[10]. Fig. 5, worth a thousand words, shows the structure function $F(x,s)$ at different values of s, defined as

$$s \equiv \ln \frac{\ln Q^2/\Lambda^2}{\ln Q_o^2/\Lambda^2}$$

The input curve is s = o. Negative (positive) s corresponds to $Q^2 < Q_o^2$ ($Q^2 > Q_o^2$). When a deviation from scaling following the pattern of the Figure is observed, Λ will be determined. Before that day one has to label the curves with values of s, rather than Q^2. If, say, Λ = 1 GeV, the curves will correspond to Q^2 = 10,20,100,2860 and 7 x 10^{18} GeV^2 in the order of decreasing area. If Λ<<1 GeV violations of scaling will be too tiny to observe. If Λ>> 1 GeV bigger accelerators or better theories are called for.

Let me now discuss the results of a theoretical ex experiment. Assume scaling to be exact in the Bloom-Gilman variable $x' = x/(1+\frac{m^2}{Q^2}x)$ and $F(x') = \sqrt{x'}(1-x')^3$. Fig. 6 then shows $F(x,Q^2)$ at different Q^2 as a function of Bjorken's original $x = Q^2/2\nu$. Except at rather

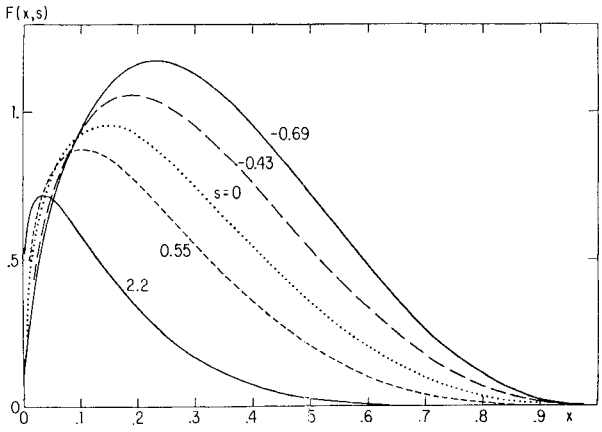

Fig. 5 The structure function F(x,s) plotted at different values of s, where $s \equiv \ell n \frac{\ell n Q^2/\Lambda^2}{\ell n Q_o^2/\Lambda^2}$

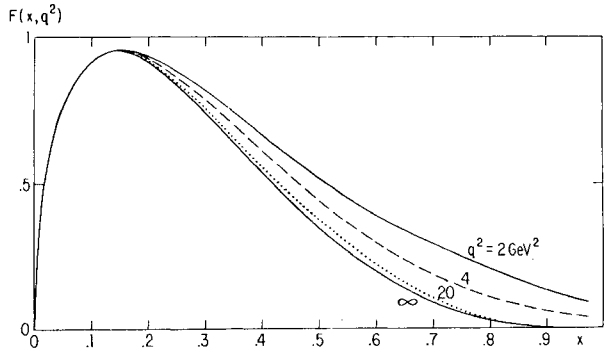

Fig. 6 Structure function $F(x,Q^2)$ as a function of Bjorken's $x \equiv Q^2/2M\nu$ under the assumption of exact scaling in the Bloom-Gilman variable $x' = x/(1 + \frac{M^2}{Q^2}x)$.

large Q^2 (10,20 GeV^2 or more) or very small x there is a breakdown of "x-scaling" not unlike the one predicted by asymptotically free field theories. Again the same warning: in the present status of the theory m^2/Q^2 corrections are not tractable, no conclusion can be drawn from the observation of low Q^2 scaling. We heard of similar conclusions, based on more elaborate experiments, in Prof. Taylor's talk in this Conference[11].

CONCLUSION: Asymptotically free field theories are not free field theories and they make non-asymptotic predictions. To understand scaling in their context we must

i) Have a good data at large Q^2, say 20-50 GeV^2.

ii) Observe a definite way in which scaling is not true.

A confirmation of the predictions may be a triumph of perturbative field theory in the realm of strong interaction dynamics.

III. Moral

In this Conference, we have heard quite a lot about monopoles, quarks, charm, coloured gluons etc. You may think that these objects exist only in our dictionaries. It is therefore appropriate to close this session with a piece of linguistic research: a photocopy of the reference[12] where the concept of "gluon" was first introduced and described (Fig.7).

REFERENCES

1. C. Rubbia. Talk presented at this Conference.
2. R. Imlay. Talk presented at this Conference.
3. See for instance J. Iliopoulos' talk at this Conference.
4. See for instance M.K. Gaillard's talk at this Conference.
5. For a titanic review, see J. Ellis' contribution to this Conference.
6. D. Gross and F. Wilczek, Phys.Rev.Letters 30, 1343 (1973)
   H.D. Politzer, Phys.Rev.Letters 30, 1346 (1973)
   G. 't Hooft (unpublished).
7. D. Gross. Talks presented at this Conference.
8. A. De Rújula, H. Georgi and H.D. Politzer. Harvard Preprint.
9. G. Parisi, Columbia preprint, March 1974.
   D J Gross, Phys. Rev. Lett. 32 (1071) 1974 .
10. S. Drell and T.M. Yan, Phys.Rev.Lett 24, 181(1970).
    G.B. West ibid 24, 1206 (1970)
    E.D. Bloom and F.J. Gilman, Phys.Rev.D4, 2901(1971)
11. R Taylor. Talk presented at this Conference.
12. "DELIRIOUS" by J. Lob and P. Douillet.

Fig. 7 Origin of the concept of "gluon".